



<b>Publication Year</b>	2019
<b>Acceptance in OA @INAF</b>	2020-12-14T10:06:09Z
<b>Title</b>	The behaviour of chemical elements in 62 Am star candidates
<b>Authors</b>	CATANZARO, Giovanni; BUSA', INNOCENZA; Gangi, Manuele Ettore; Giarrusso, M.; LEONE, FRANCESCO; et al.
<b>DOI</b>	10.1093/mnras/stz080
<b>Handle</b>	<a href="http://hdl.handle.net/20.500.12386/28814">http://hdl.handle.net/20.500.12386/28814</a>
<b>Journal</b>	MONTHLY NOTICES OF THE ROYAL ASTRONOMICAL SOCIETY
<b>Number</b>	484

# The behaviour of chemical elements in 62 Am star candidates

G. Catanzaro<sup>1</sup>,<sup>1</sup>★ I. Busà,<sup>1</sup> M. Gangi,<sup>2</sup> M. Giarrusso<sup>1</sup>,<sup>3</sup> F. Leone<sup>1,2</sup> and M. Munari<sup>1</sup>

<sup>1</sup>INAF – Osservatorio Astrofisico di Catania, Via S. Sofia 78, I-95123 Catania, Italy

<sup>2</sup>Università degli studi di Catania, Via S. Sofia 78, I-95123 Catania, Italy

<sup>3</sup>INFN Laboratori Nazionali del Sud, Via S. Sofia 62, I-95123 Catania, Italy

Accepted 2018 December 30. Received 2018 December 30; in original form 2018 November 15

## ABSTRACT

In this paper, we present the results of a spectroscopic campaign devoted to ascertain the actual nature of a sample of 155 objects reported as uncertain peculiar stars in the General catalogue of Ap, Am, and HgMn stars. Spectroscopic observations have been obtained with Catania Astrophysical Observatory Spectropolarimeter. We derive for all the objects that appear to be single stars, effective temperature, gravity, rotational and radial velocities, and chemical abundances by spectral synthesis method, then by using an abundance-based criterion we selected 62 Am star candidates. Further, by using the positions of these stars within the theoretical instability strips for  $\delta$  Sct and  $\gamma$  Dor in the Hertzsprung–Russell diagram, we selected 46 out of 62 candidates to be possible pulsating stars, in particular 42 are candidates  $\delta$  Sct and four candidates hybrid stars.

**Key words:** stars: abundances – stars: chemically peculiar – stars: early-type – stars: fundamental parameters.

## 1 INTRODUCTION

Main-sequence chemically peculiar stars (hereafter CP stars) are objects that show anomalies in their chemical composition if compared to stars with the same effective temperature. Among them, the Am subgroup shows Ca II K-line too early for their hydrogen line types, while metallic lines appear too late, such that the spectral types inferred from the Ca II K- and metal lines differ by five or more spectral subclasses. The marginal Am stars (denoted with Am:) are those whose difference between Ca II K- and metal lines is less than five subclasses. The commonly used classification for this class of objects includes three spectral types prefixed with k, h, and m, corresponding to the K-line, hydrogen lines, and metallic lines, respectively. The typical chemical pattern shows underabundances of Ca and/or Sc and overabundances of the Fe-peak elements, Y, Ba, and of rare earths elements (Catanzaro & Balona 2012; Catanzaro, Ripepi & Bruntt 2013; Catanzaro & Ripepi 2014; Catanzaro et al. 2015).

One of the most exhaustive catalogue of peculiar stars is the General Catalogue of Ap and Am stars by Renson & Manfroid (2009), in which 8205 peculiar (or suspected peculiar) stars are included. Among these, 3652 are Ap (or probably Ap) stars, 162 are HgMn (or probable), 4299 Am (or probable), and 92 stars that have been wrongly catalogued at least once as Ap, HgMn, or Am. In the catalogue, stars are marked with a flag indicating the degree of confidence for their CP nature. In particular, a slash (/) indicates

a star that was improperly considered to have an Ap, HgMn, or Am nature, a question mark (?) means doubtful cases (2314 stars), and ‘blank’ all the other cases. On the contrary asterisk (\*) denotes well-known confirmed Ap, HgMn, or Am stars (only 426).

The primary aim of this work was to provide the most detailed and homogeneous classification possible, for stars that are listed as uncertain in the Renson & Manfroid (2009) catalogue. To achieve this goal, in 2014 we undertook an observational campaign using the facilities of the Catania Astrophysical Observatory (see Section 2). The only criterion used for selecting stars, in addition to their observability, was to choose stars with  $V \leq 10$  in order to obtain spectra with a signal-to-noise ratio (S/N)  $\geq 100$  with reasonable exposure times ( $T_{\text{exp}} \leq 45$  min).

From the whole sample of doubtful stars, 26 per cent of them have  $V > 10$  and therefore are too faint to be observable with our telescope. About the remaining stars, we have excluded a further 47 per cent as they have  $\text{Dec.} \leq -25^\circ$  and then not observable from Catania latitude. Given these criteria, the remaining number of observable uncertain stars is 788.

We observed 155 stars in total so far, even if we excluded 29 objects as at a first glance they showed spectral signatures typical of double line spectroscopic binary (SB2) systems. For the remaining 126 stars (see Table 1), we estimated the principal astrophysical parameters such as effective temperature, gravity, rotational and radial velocity, and chemical abundances of principal elements. From this sample we selected only the stars that show typical Am signature in their chemical pattern (62 in total) and for them we present detailed chemical abundances. For the remaining 64 stars

\* E-mail: [gca@oact.inaf.it](mailto:gca@oact.inaf.it)

**Table 1.** For each observed star we report HD number, effective temperature and surface gravity both derived by spectral energy distribution (SED) analysis performed by using Virtual Observatory SED Analyzer (VOSA) and from spectral synthesis, radial and projected rotational velocities, and Heliocentric Julian Date (HJD) of the observation.

Name	$T_{\text{eff}}^{\text{VOSA}}$ (K)	$\log g^{\text{VOSA}}$	$T_{\text{eff}}$ (K)	$\log g$	$v \sin i$ (km s <sup>-1</sup> )	RV (km s <sup>-1</sup> )	HJD (240 0000. +)
HD 267	7750 ± 125	4.00 ± 0.25	8200 ± 125	4.0 ± 0.25	62 ± 5	0.6 ± 1.5	57271.533
HD 1732	7600 ± 125	4.00 ± 0.25	8250 ± 150	3.5 ± 0.25	13 ± 1	6.0 ± 0.2	57993.573
HD 2523	7000 ± 125	4.00 ± 0.25	7750 ± 150	3.5 ± 0.25	38 ± 4	20.8 ± 0.5	57610.591
HD 2887	8250 ± 125	3.50 ± 0.25	8700 ± 125	4.3 ± 0.25	35 ± 3	-1.8 ± 0.5	57272.539
HD 3992	8000 ± 125	4.00 ± 0.25	8500 ± 150	4.0 ± 0.25	193 ± 20	10.0 ± 1.2	56910.568
HD 4186	8250 ± 125	4.00 ± 0.25	7750 ± 150	4.0 ± 0.25	20 ± 2	15.6 ± 0.2	57278.531
HD 6164	7500 ± 125	3.50 ± 0.25	8000 ± 125	3.5 ± 0.25	21 ± 2	-6.3 ± 0.1	57993.603
HD 7025	8400 ± 125	4.00 ± 0.25	8750 ± 150	3.5 ± 0.25	69 ± 7	6.2 ± 1.0	57271.559
HD 8251	7000 ± 125	4.50 ± 0.25	7300 ± 125	4.0 ± 0.25	32 ± 3	12.5 ± 0.7	57278.556
HD 10088	8000 ± 125	3.50 ± 0.25	7700 ± 125	4.0 ± 0.25	40 ± 3	12.3 ± 1.3	57272.582
HD 10186	7500 ± 125	4.00 ± 0.25	8250 ± 150	3.5 ± 0.25	69 ± 7	0.5 ± 2.0	57271.583
HD 13248	8250 ± 125	3.50 ± 0.25	7800 ± 125	4.0 ± 0.25	18 ± 1	16.7 ± 0.5	56907.596
HD 14825	8000 ± 125	4.00 ± 0.25	8500 ± 125	4.0 ± 0.25	71 ± 5	-19.9 ± 0.3	57278.591
HD 18346	8300 ± 125	3.80 ± 0.25	7750 ± 150	4.0 ± 0.25	13 ± 1	-28.8 ± 0.6	57271.636
HD 20118	7600 ± 125	4.00 ± 0.25	7250 ± 150	4.0 ± 0.25	62 ± 6	27.2 ± 0.7	57272.636
HD 99620	8000 ± 125	3.50 ± 0.25	7700 ± 125	4.0 ± 0.25	40 ± 3	-9.1 ± 0.9	56757.429
HD 104241	8800 ± 125	4.00 ± 0.25	8750 ± 150	3.5 ± 0.25	92 ± 9	-22.1 ± 1.2	56818.319
HD 108408	8250 ± 125	3.00 ± 0.25	8500 ± 150	3.5 ± 0.25	60 ± 6	-22.6 ± 1.1	57149.380
HD 108449	6750 ± 125	4.00 ± 0.25	7000 ± 125	4.0 ± 0.25	60 ± 5	14.9 ± 0.5	56805.313
HD 110248	7700 ± 125	3.50 ± 0.25	7750 ± 150	3.5 ± 0.25	17 ± 2	-9.5 ± 0.2	57162.346
HD 115708	7250 ± 125	3.50 ± 0.25	8250 ± 150	3.5 ± 0.25	13 ± 1	4.0 ± 0.7	56820.312
HD 117624	7000 ± 125	3.50 ± 0.25	7500 ± 125	4.0 ± 0.25	18 ± 1	21.2 ± 1.1	56812.336
HD 120049	7000 ± 125	4.00 ± 0.25	7200 ± 125	4.0 ± 0.25	63 ± 5	29.8 ± 0.5	56805.365
HD 122911	7000 ± 125	4.00 ± 0.25	7750 ± 150	3.5 ± 0.25	38 ± 4	-24.4 ± 0.9	56757.505
HD 124954	7250 ± 125	4.00 ± 0.25	7200 ± 125	3.5 ± 0.25	42 ± 3	18.2 ± 0.3	56792.422
HD 127263	8250 ± 125	3.50 ± 0.25	8200 ± 125	4.0 ± 0.25	10 ± 1	-31.6 ± 0.0	57934.325
HD 130771	7750 ± 125	3.50 ± 0.25	7300 ± 125	4.0 ± 0.25	29 ± 2	-15.1 ± 1.5	56820.359
HD 132295	7750 ± 125	3.50 ± 0.25	7300 ± 125	4.0 ± 0.25	65 ± 5	16.5 ± 0.4	56819.371
HD 132739	6800 ± 125	4.00 ± 0.25	8250 ± 150	3.5 ± 0.25	19 ± 2	26.8 ± 1.5	56812.387
HD 133157	7300 ± 125	4.00 ± 0.25	8000 ± 150	3.5 ± 0.25	63 ± 6	-26.3 ± 2.0	56813.391
HD 134214	8000 ± 125	3.50 ± 0.25	7500 ± 125	3.5 ± 0.25	9 ± 1	10.9 ± 0.4	57189.359
HD 139939	8250 ± 125	4.00 ± 0.25	7800 ± 125	3.6 ± 0.25	31 ± 3	-22.1 ± 0.4	56756.590
HD 142070	8800 ± 125	4.40 ± 0.25	8250 ± 150	3.5 ± 0.25	11 ± 1	-8.7 ± 0.2	57920.400
HD 143898	8000 ± 125	3.50 ± 0.25	7500 ± 125	4.0 ± 0.25	18 ± 1	3.9 ± 0.4	57149.515
HD 143914	7500 ± 125	4.00 ± 0.25	8000 ± 125	4.0 ± 0.25	49 ± 4	-16.4 ± 1.0	57934.358
HD 144463	6200 ± 125	4.00 ± 0.25	10000 ± 150	4.0 ± 0.25	9 ± 1	9.4 ± 0.2	57574.392
HD 144999	7900 ± 125	3.50 ± 0.25	8250 ± 150	3.5 ± 0.25	8 ± 1	-26.3 ± 0.3	56852.327
HD 147275	7000 ± 125	4.00 ± 0.25	8250 ± 150	3.5 ± 0.25	46 ± 5	-10.8 ± 0.4	56813.446
HD 148980	7250 ± 125	4.50 ± 0.25	7200 ± 125	4.0 ± 0.25	73 ± 5	3.3 ± 0.6	56858.344
HD 149650	8500 ± 125	3.50 ± 0.25	8800 ± 125	4.0 ± 0.25	104 ± 10	-8.2 ± 1.0	57570.389
HD 149748	8000 ± 125	3.50 ± 0.25	7600 ± 125	4.0 ± 0.25	37 ± 3	-21.0 ± 0.8	57570.411
HD 150391	8500 ± 125	4.00 ± 0.25	8250 ± 150	3.5 ± 0.25	90 ± 9	-23.3 ± 1.5	57934.390
HD 153450	8000 ± 125	4.00 ± 0.25	8500 ± 150	3.5 ± 0.25	5 ± 1	-29.4 ± 0.2	57933.397
HD 154225	5700 ± 125	4.00 ± 0.25	7250 ± 150	3.5 ± 0.25	8 ± 1	-8.9 ± 1.6	56791.551
HD 154226	7500 ± 125	4.00 ± 0.25	7800 ± 125	4.5 ± 0.25	39 ± 3	8.7 ± 0.4	57149.554
HD 155316	7750 ± 125	4.00 ± 0.25	7600 ± 125	3.5 ± 0.25	40 ± 3	3.5 ± 0.6	57567.422
HD 158116	7800 ± 125	3.00 ± 0.25	8000 ± 150	3.5 ± 0.25	19 ± 2	-24.6 ± 0.4	56857.391
HD 158450	8700 ± 125	4.00 ± 0.25	8250 ± 150	3.5 ± 0.25	24 ± 2	-15.6 ± 0.4	57933.429
HD 159545	8250 ± 125	4.00 ± 0.25	8700 ± 125	3.5 ± 0.25	30 ± 3	12.9 ± 3.3	56813.531
HD 161370	8800 ± 125	4.00 ± 0.25	8500 ± 150	3.5 ± 0.25	102 ± 10	-17.0 ± 0.8	56840.435
HD 161660	13000 ± 125	3.50 ± 0.25	12500 ± 125	3.7 ± 0.25	25 ± 2	-15.3 ± 1.6	58268.501
HD 162705	7300 ± 125	4.00 ± 0.25	8000 ± 150	3.5 ± 0.25	52 ± 5	-16.5 ± 0.7	56851.419
HD 163422	8500 ± 125	3.50 ± 0.25	8500 ± 125	3.5 ± 0.25	80 ± 6	-14.5 ± 0.7	57567.391
HD 164394	7500 ± 125	4.50 ± 0.25	7700 ± 125	3.5 ± 0.25	92 ± 7	-0.9 ± 0.7	56852.413
HD 165474	8400 ± 125	3.80 ± 0.25	8500 ± 150	3.5 ± 0.25	10 ± 1	14.2 ± 0.6	57220.406
HD 166016	8000 ± 125	4.00 ± 0.25	8500 ± 125	3.0 ± 0.25	90 ± 7	-15.4 ± 3.5	56875.358
HD 166894	8500 ± 125	3.50 ± 0.25	8750 ± 125	4.0 ± 0.25	52 ± 4	-13.0 ± 0.4	56818.562
HD 167828	9000 ± 125	4.00 ± 0.25	8750 ± 125	4.0 ± 0.25	26 ± 2	-12.2 ± 0.3	56858.423
HD 168071	8750 ± 125	4.50 ± 0.25	8500 ± 150	3.5 ± 0.25	8 ± 1	-26.2 ± 0.2	57920.497
HD 168796	8750 ± 125	4.50 ± 0.25	8500 ± 125	4.0 ± 0.25	13 ± 1	16.4 ± 0.2	57179.513
HD 169885	8250 ± 125	3.50 ± 0.25	8500 ± 125	3.8 ± 0.25	39 ± 3	-4.4 ± 0.7	57570.471
HD 170054	11250 ± 125	4.50 ± 0.25	11700 ± 125	3.8 ± 0.25	25 ± 2	-14.6 ± 0.8	57934.480
HD 170563	7500 ± 125	4.00 ± 0.25	7100 ± 125	4.0 ± 0.25	31 ± 2	-24.6 ± 0.2	58270.576

**Table 1** – *continued*

Name	$T_{\text{eff}}^{\text{VOSA}}$ (K)	$\log g^{\text{VOSA}}$	$T_{\text{eff}}$ (K)	$\log g$	$v \sin i$ ( $\text{km s}^{-1}$ )	RV ( $\text{km s}^{-1}$ )	HJD (240 0000. +)
HD 170901	10000 ± 125	4.00 ± 0.25	9750 ± 125	4.0 ± 0.25	194 ± 20	10.4 ± 1.5	57933.491
HD 171363	7500 ± 125	4.50 ± 0.25	7600 ± 125	4.0 ± 0.25	17 ± 1	−14.8 ± 0.2	56846.502
HD 171782	9250 ± 125	4.00 ± 0.25	9200 ± 125	3.5 ± 0.25	25 ± 2	15.7 ± 0.6	56839.498
HD 171914	11250 ± 125	3.50 ± 0.25	11800 ± 125	3.8 ± 0.25	50 ± 4	−14.2 ± 0.8	56839.521
HD 172403	11500 ± 125	4.00 ± 0.25	7750 ± 150	4.0 ± 0.25	25 ± 2	−4.5 ± 1.2	56852.495
HD 172713	6500 ± 125	4.00 ± 0.25	8500 ± 150	3.5 ± 0.25	7 ± 1	−8.9 ± 0.3	57603.412
HD 173654B	7500 ± 125	4.00 ± 0.25	8500 ± 150	3.5 ± 0.25	14 ± 1	13.8 ± 0.3	56858.459
HD 174646	7300 ± 125	4.00 ± 0.25	8250 ± 150	3.5 ± 0.25	25 ± 2	−5.5 ± 0.6	57234.413
HD 174704	7000 ± 125	4.00 ± 0.25	8500 ± 150	3.5 ± 0.25	8 ± 1	−32.7 ± 0.3	56857.440
HD 176716	7750 ± 125	3.50 ± 0.25	8200 ± 125	4.0 ± 0.25	68 ± 5	−9.2 ± 0.6	57920.533
HD 177645	7200 ± 125	4.00 ± 0.25	8500 ± 150	3.5 ± 0.25	24 ± 2	5.1 ± 0.7	56839.543
HD 179461	7100 ± 125	4.00 ± 0.25	8500 ± 150	3.5 ± 0.25	14 ± 1	−14.5 ± 1.2	56851.484
HD 179892	8000 ± 125	3.50 ± 0.25	7700 ± 125	3.5 ± 0.25	86 ± 6	−0.9 ± 4.8	56874.425
HD 180347	8000 ± 125	4.50 ± 0.25	7600 ± 125	4.0 ± 0.25	11 ± 1	5.1 ± 0.1	56912.316
HD 181206	7600 ± 125	4.00 ± 0.25	9000 ± 150	3.5 ± 0.25	80 ± 8	−16.0 ± 1.2	56912.352
HD 182381	8750 ± 125	3.00 ± 0.25	8500 ± 150	3.5 ± 0.25	60 ± 6	−12.0 ± 1.6	56846.568
HD 183489	7200 ± 125	4.00 ± 0.25	7500 ± 150	3.5 ± 0.25	93 ± 9	−24.5 ± 2.0	56907.323
HD 184903	9750 ± 125	3.50 ± 0.25	9300 ± 125	4.0 ± 0.25	89 ± 7	−14.4 ± 1.6	57933.564
HD 185330	13200 ± 125	3.30 ± 0.25	9500 ± 150	3.5 ± 0.25	7 ± 1	−28.8 ± 0.7	57570.505
HD 187128	9000 ± 125	3.50 ± 0.25	9000 ± 300	4.0 ± 0.25	17 ± 1	−21.3 ± 0.9	56840.576
HD 187192	10000 ± 125	2.90 ± 0.25	10250 ± 150	3.5 ± 0.25	30 ± 3	−13.9 ± 0.6	56851.516
HD 187258	6800 ± 125	3.00 ± 0.25	8500 ± 150	3.5 ± 0.25	11 ± 1	−24.4 ± 0.2	56839.574
HD 187959	8250 ± 125	3.50 ± 0.25	7800 ± 125	4.0 ± 0.25	43 ± 4	−25.2 ± 0.3	57598.459
HD 188041	8400 ± 125	3.90 ± 0.25	8250 ± 150	3.5 ± 0.25	9 ± 1	−21.0 ± 1.3	57220.467
HD 188103	9500 ± 125	3.50 ± 0.25	9500 ± 125	3.0 ± 0.25	45 ± 4	−22.9 ± 0.8	56852.545
HD 188854	6750 ± 125	3.50 ± 0.25	7200 ± 125	4.0 ± 0.25	10 ± 1	−27.5 ± 0.9	56839.600
HD 189574	7500 ± 125	3.50 ± 0.25	7500 ± 125	4.0 ± 0.25	37 ± 3	−13.2 ± 1.4	56907.352
HD 189652	6700 ± 125	4.00 ± 0.25	7750 ± 150	3.5 ± 0.25	55 ± 5	28.2 ± 0.6	56851.562
HD 190068	8750 ± 125	3.00 ± 0.25	9500 ± 150	3.5 ± 0.25	25 ± 2	−22.4 ± 1.0	56910.361
HD 190145	7750 ± 125	3.50 ± 0.25	7500 ± 125	4.0 ± 0.25	13 ± 1	−13.9 ± 0.3	56819.598
HD 190850	8000 ± 125	3.50 ± 0.25	8500 ± 125	4.0 ± 0.25	158 ± 16	−22.9 ± 1.1	56857.521
HD 192124	8250 ± 125	3.50 ± 0.25	8250 ± 150	3.5 ± 0.25	75 ± 7	18.0 ± 2.0	56858.548
HD 192541	7250 ± 125	3.50 ± 0.25	7700 ± 125	4.0 ± 0.25	47 ± 4	−42.0 ± 0.4	57941.540
HD 192662	8250 ± 125	4.50 ± 0.25	8400 ± 125	4.0 ± 0.25	45 ± 4	−6.7 ± 0.6	56910.401
HD 194822	7300 ± 125	4.00 ± 0.25	8000 ± 150	3.5 ± 0.25	35 ± 3	10.7 ± 1.5	56875.453
HD 195490	7400 ± 125	4.00 ± 0.25	7750 ± 150	3.5 ± 0.25	22 ± 2	−35.3 ± 0.7	56907.392
HD 198406	8000 ± 125	3.50 ± 0.25	7800 ± 125	4.0 ± 0.25	80 ± 6	35.8 ± 0.5	57234.506
HD 199180	9000 ± 125	4.00 ± 0.25	8500 ± 125	3.5 ± 0.25	9 ± 1	−16.3 ± 0.9	56875.507
HD 202431	7500 ± 125	4.00 ± 0.25	7300 ± 125	4.0 ± 0.25	9 ± 1	12.1 ± 0.1	57597.594
HD 203786	11700 ± 125	4.00 ± 0.25	9500 ± 150	4.0 ± 0.25	20 ± 2	3.8 ± 0.5	57941.571
HD 206028	11000 ± 125	3.50 ± 0.25	12500 ± 150	4.0 ± 0.25	39 ± 4	−19.1 ± 2.0	56857.551
HD 207188	9250 ± 125	3.50 ± 0.25	10000 ± 125	3.5 ± 0.25	45 ± 4	−9.8 ± 0.7	56907.431
HD 209147	8800 ± 125	4.00 ± 0.25	7750 ± 150	3.5 ± 0.25	80 ± 8	−11.9 ± 1.8	57272.452
HD 209639	7200 ± 125	4.00 ± 0.25	8250 ± 150	3.5 ± 0.25	80 ± 8	−13.1 ± 1.8	56932.396
HD 209711	7500 ± 125	4.00 ± 0.25	8250 ± 150	3.5 ± 0.25	65 ± 6	0.1 ± 2.0	56932.434
HD 209947	6900 ± 125	4.00 ± 0.25	7500 ± 150	3.5 ± 0.25	40 ± 4	11.5 ± 0.5	56910.453
HD 210432	8700 ± 125	4.00 ± 0.25	8500 ± 150	3.5 ± 0.25	165 ± 5	−7.1 ± 0.4	57272.476
HD 210433	9500 ± 125	4.00 ± 0.25	9000 ± 125	4.5 ± 0.25	29 ± 3	−9.7 ± 0.3	57272.476
HD 211099	10500 ± 125	3.50 ± 0.25	10500 ± 150	3.5 ± 0.25	33 ± 3	−2.9 ± 1.4	56874.528
HD 211643	8250 ± 125	3.50 ± 0.25	8700 ± 125	4.0 ± 0.25	64 ± 5	−14.5 ± 0.8	57603.597
HD 211785	7800 ± 125	4.00 ± 0.25	8250 ± 150	3.5 ± 0.25	26 ± 3	−4.3 ± 0.5	56947.349
HD 211906	7750 ± 125	3.50 ± 0.25	7500 ± 125	4.0 ± 0.25	23 ± 2	−28.7 ± 0.3	57993.477
HD 213143	7300 ± 125	4.00 ± 0.25	7750 ± 150	3.5 ± 0.25	8 ± 1	11.5 ± 0.1	56857.596
HD 215327	8250 ± 125	3.50 ± 0.25	8300 ± 125	3.5 ± 0.25	13 ± 1	−7.4 ± 0.1	56944.372
HD 216018	7200 ± 125	4.00 ± 0.25	9000 ± 150	3.5 ± 0.25	11 ± 1	−1.7 ± 0.3	57959.587
HD 218395	8000 ± 125	4.00 ± 0.25	9250 ± 150	3.5 ± 0.25	200 ± 20	−21.1 ± 0.3	57271.481
HD 220668	11500 ± 125	4.00 ± 0.25	11100 ± 125	3.3 ± 0.25	25 ± 1	−9.5 ± 0.1	57278.465
HD 221568	7000 ± 125	4.00 ± 0.25	8500 ± 150	3.5 ± 0.25	6 ± 1	−7.1 ± 2.0	56943.390
HD 223531	8500 ± 125	4.50 ± 0.25	8800 ± 125	3.9 ± 0.25	27 ± 2	−8.7 ± 0.6	56874.629
HD 223660	10700 ± 125	3.30 ± 0.25	9000 ± 150	3.5 ± 0.25	17 ± 2	−11.2 ± 0.7	57278.490
HD 224002	8000 ± 200	3.50 ± 0.25	7600 ± 125	4.0 ± 0.25	33 ± 3	−0.8 ± 0.5	57993.534
HD 224657	7000 ± 125	4.00 ± 0.25	7000 ± 125	4.0 ± 0.25	61 ± 5	−25.0 ± 1.9	56874.589
HD 225137	8400 ± 125	3.80 ± 0.25	8500 ± 150	3.5 ± 0.25	20 ± 2	−38.9 ± 0.8	57272.515

not classified as Am stars, we refer the reader to a forthcoming paper.

In the meantime, the observations are still ongoing, so we plan to obtain spectra for all of the selected stars in a few years.

## 2 OBSERVATIONS AND DATA REDUCTION

Spectroscopic observations of our sample of stars, listed in Table 1, were carried out with the Catania Astrophysical Observatory Spectropolarimeter (CAOS) that is a fibre-fed, high-resolution, cross-dispersed echelle spectrograph (Leone et al. 2016) installed at the Cassegrain focus of the 91-cm telescope of the M. G. Fracastoro observing station of the Catania Astrophysical Observatory (Mt Etna, Italy).

Our spectra were obtained between 2014 April and 2018 May, exposure times have been tuned in order to obtain for the stars a S/N of at least 100 in the continuum in the 3900–6800 Å spectral range, with a resolution of  $R = 45\,000$ , as measured from ThAr and telluric lines.

The reduction of all spectra, which included the subtraction of the bias frame, trimming, correcting for the flat-field and the scattered light, extraction for the orders, and wavelength calibration, was done using the National Optical Astronomy Observatory (NOAO)/IRAF packages. Given the importance of Balmer lines in our analysis, we paid much more attention to the normalization of the corresponding spectral orders. In particular, we divided the spectral order containing H $\alpha$  and H $\beta$  by a pseudo-continuum obtained combining the continua of the previous and subsequent echelle orders, as already outlined by Catanzaro et al. (2015). The IRAF package RVCORRECT was used to determine the barycentric velocity and correct the observed radial velocities for the Earth’s motion.

## 3 ATMOSPHERIC PARAMETERS

In order to proceed with our aim to select from this sample only the Am stars, we have to derive the chemical abundances. For this purpose, we need to estimate fundamental astrophysical quantities, such as effective temperatures, surface gravities, and rotational and radial velocities. The approach used in this paper has been successfully used in other papers devoted to this topic (see e.g. Catanzaro & Balona 2012; Catanzaro et al. 2013; Catanzaro & Ripepi 2014; Catanzaro et al. 2015).

As a first guess, we estimated effective temperature and surface gravity by comparing the observed spectral energy distribution (SED) with synthetic spectra. To this aim we adopted the Virtual Observatory SED Analyzer (VOSA) tool (Bayo et al. 2008). The major sources of photometry, used by VOSA for collecting data, were the Tycho-2 (Høg et al. 2000), Two Micron All-Sky Survey (2MASS; Skrutskie et al. 2006), and *Wide-field Infrared Survey Explorer* (WISE; Wright et al. 2010) catalogues, complemented with Strömgren (Paunzen 2015), Sloan (Brown et al. 2011), and *Galaxy Evolution Explorer* (GALEX)<sup>1</sup> photometry. VOSA performed a least-square fit to this SED by using a grid of ATLAS9 Kurucz ODFNEW/NOVER models (Castelli, Gratton & Kurucz 1997) to obtain a first estimate of temperature and gravity. For this fit we choose to keep the metallicity fixed to solar values (Grevesse & Sauval 1998). Results of VOSA have reported in columns 3 and 4 of Table 1.

These values have been used as starting guesses for an iterative procedure aimed at minimizing the difference among observed and

synthetic spectra, using as goodness-of-fit parameter the  $\chi^2$  defined as

$$\chi^2 = \frac{1}{N} \sum \left( \frac{I_{\text{obs}} - I_{\text{th}}}{\delta I_{\text{obs}}} \right)^2, \quad (1)$$

where  $N$  is the total number of points,  $I_{\text{obs}}$  and  $I_{\text{th}}$  are the intensities of the observed and computed profiles, respectively, and  $\delta I_{\text{obs}}$  is the photon noise. Synthetic spectra were generated in three steps: (i) we computed local thermodynamic equilibrium (LTE) atmospheric models using the ATLAS9 code (Kurucz 1993a,b); (ii) the stellar spectra were synthesized using SYNTHE (Kurucz & Avrett 1981); and (iii) the spectra were convolved for the instrumental and rotational broadening.

We computed the  $v \sin i$  of our targets by matching synthetic lines profiles from SYNTHE to a selected set of metal lines, in particular we used the Mg I triplet at  $\lambda\lambda 5167\text{--}5183$  Å for the cooler stars of our sample ( $T_{\text{eff}} \leq 9000$  K) and the Mg II 4481 Å for the hottest ( $T_{\text{eff}} > 9000$  K). The radial velocities have been measured by cross-correlating each observed spectrum with a synthetic one. The cross-correlation has been calculated by means of the IRAF task FXCOR excluding Balmer lines and intervals with telluric lines. The resulting  $v \sin i$  and radial velocity values, together with the heliocentric Julian date of the observation, are listed in the last three columns of Table 1.

To determine stellar parameters as consistently as possible with the actual structure of the atmosphere, we adopted the following iterative procedure to perform the abundances analysis.

(i)  $T_{\text{eff}}$  was estimated by computing the ATLAS9 model atmosphere that produces the best match between the observed H $\alpha$  and H $\beta$  lines profile and those computed with SYNTHE. As a first iteration, models were computed using solar opacity distribution functions (ODFs) and  $T_{\text{eff}}$  and  $\log g$  derived with VOSA. In our spectra, H $\alpha$  and H $\beta$  are located far from the echelle order edges so that it was possible to safely recover the whole profile. The simultaneous fitting of these two lines led to a final solution as the intersection of the two  $\chi^2$  isosurfaces. An important source of uncertainties arises from the difficulties in continuum normalization as it is always challenging for Balmer lines in echelle spectra. We quantified the error introduced by the normalization to be at least 100 K that we summed in quadrature with the errors obtained by the fitting procedure. The final results for effective temperatures and their errors are reported in Table 1. Uncertainties in  $T_{\text{eff}}$ ,  $\log g$ , and  $v \sin i$  as shown in Table 1 were estimated by the change in parameter values that leads to an increases of  $\chi^2$  by unity (Lampton, Margon & Bowyer 1976). Microturbulence velocities have been estimated by using the calibration given by Gebran et al. (2014).

(ii) As a second step we determined the abundances of individual species by spectral synthesis. Therefore, we divided spectra into several intervals, 50 Å wide each, and derived the abundances in each interval by performing a  $\chi^2$  minimization of the difference between the observed and synthetic spectrum. The minimization algorithm has been written in IDL<sup>2</sup> language, using the AMOEBA routine. We adopted lists of spectral lines and atomic parameters from Castelli & Hubrig (2004), who updated the parameters listed originally by Kurucz & Bell (1995). Errors on abundances have been quantified by combining in quadrature the standard deviation and the uncertainties coming from atmospheric parameters.

<sup>2</sup>IDL (Interactive Data Language) is a registered trademark of Harris Geospatial Solutions.

<sup>1</sup><http://galex.stsci.edu/GR6/>



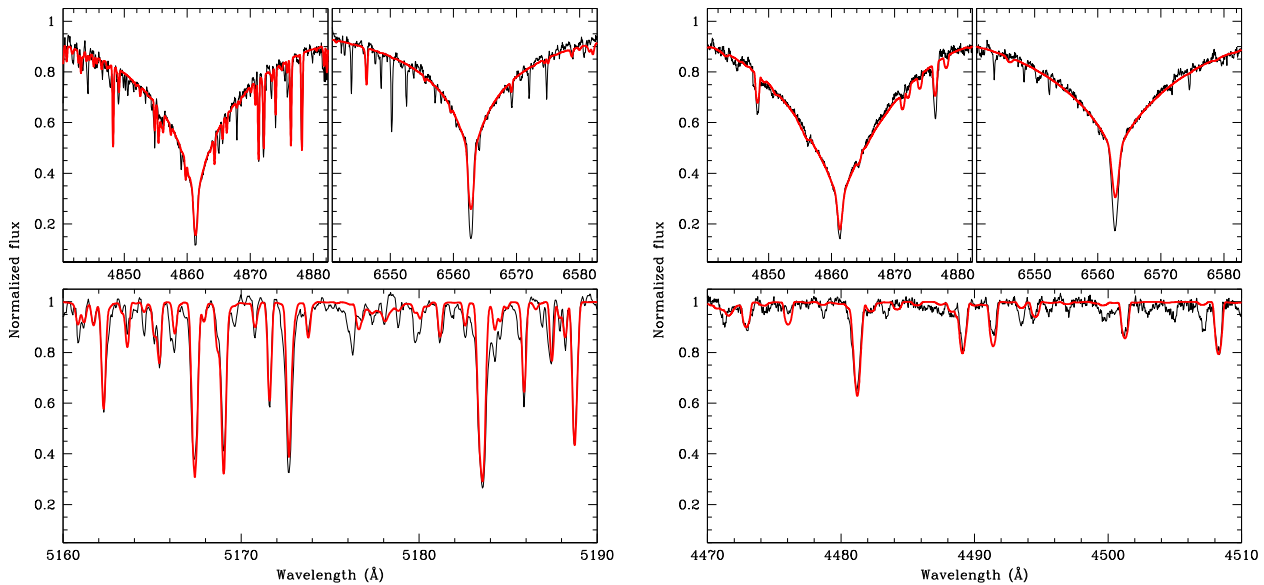


**Figure 1.** Examples of results of our procedure for HD 134214 (left-hand panel) and HD 171782 (right-hand panel). For each star, we show the observed spectrum (black line) overimposed to the synthetic one (red line) with the atmospheric parameters listed in Table 1.  $H\alpha$  and  $H\beta$  are displayed for both stars, while for the coldest one (HD 134214) we plotted the spectral region around Mg I triplet at  $\lambda\lambda$  5167–5183 Å and for the hottest the region around Mg I  $\lambda$ 4481 Å. All the narrow features present in the observed spectra and not fitted by our models are telluric lines.

As an example of results obtained with this procedure, we show in Fig. 1 the synthetic spectra computed for two stars having different effective temperatures: HD 134214 ( $T_{\text{eff}} = 7500 \pm 125$  K) and HD 171782 ( $T_{\text{eff}} = 9200 \pm 125$  K).

#### 4 SELECTION AND ABUNDANCES OF AM STARS

To select the candidate Am stars among all the objects we observed, we have first established a criterion for the analysis.

We proceed as follows. First, we collected a number of well-known Am stars whose abundances have been already classified in the literature. In particular we used papers by Catanzaro et al. (2013, 2015), Niemczura et al. (2015), Catanzaro & Ripepi (2014), Catanzaro & Balona (2012), and Yuce & Adelman (2014), from which we obtained abundances for  $\approx 130$  Am stars. From these stars we considered the abundances of those elements that are characteristic for the Am stars, Ca, Sc, and iron-peak elements such as Ti, Cr, Mn, and Fe. Finally, we adopted the distribution of their abundances as a benchmark for the selection of candidates Am stars among our sample.

In Fig. 2, red histograms and red lines show the distribution of abundances (with respect to the Sun) for known Am stars and their Gaussian fit, respectively. Average values are

$$\begin{aligned} \langle [\text{Ca}] \rangle &= -0.30 \pm 0.05, \\ \langle [\text{Sc}] \rangle &= -0.47 \pm 0.06, \\ \langle [\text{Ti}] \rangle &= 0.14 \pm 0.03, \\ \langle [\text{Cr}] \rangle &= 0.37 \pm 0.03, \\ \langle [\text{Mn}] \rangle &= 0.28 \pm 0.03, \\ \langle [\text{Fe}] \rangle &= 0.33 \pm 0.02. \end{aligned}$$

We used these values as thresholds for selecting Am stars in our sample, in the sense that all the stars that have calcium and/or scandium under the respective values and, at the same time, iron-peak abundances above their threshold. In Fig. 2, this procedure

is shown by means of histograms: light blue histograms refer to the distribution of abundances for all the stars, while dark blue histograms are the distributions for the identified Am stars, whose list is reported in Table 2.

After the selection, we computed average chemical abundances for 29 species for which spectral lines have been detected in the spectra. These values are reported in Table 3 and plotted in Fig. 3. Abundances for single species for every star have been reported in Table A1. For each element we reported the abundance, relative to the solar value (Grevesse et al. 2010), and the total uncertainty; dashes mean that no spectral lines have been detected for that specie.

Rotational velocity is one of the fundamental parameters that influence stellar evolution. Stellar rotation strongly depends on spectral type; the earlier the spectral type, the faster the star rotates (Abt 2009; Royer 2009). Abt (2000) pointed out that most of the standard stars in the spectral range A0 V–F0 V have equatorial velocities greater than  $120 \text{ km s}^{-1}$ . For the same spectral type, the velocities decrease drastically in the case of the peculiar stars (see e.g. Niemczura et al. 2015). This is confirmed by the velocities inferred for our stars, their values ranging from 8 to  $104 \text{ km s}^{-1}$ , with most of them ( $\approx 67$  per cent) have  $v \sin i < 48 \text{ km s}^{-1}$  as it is shown in the histogram plotted in top panel of Fig. 4.

The distribution of spectroscopic temperatures for the selected Am stars is shown in the histogram plotted in the bottom panel of Fig. 4. The histogram peaks at  $\approx 7500$  K (around spectral type A9), which is typical for Am stars. Only five objects exceed the temperature of 10 000 K.

It is useful to compare the values of  $T_{\text{eff}}$  derived spectroscopically with those obtained via SED fitting. Inspection of Fig. 5, which illustrates such a comparison, shows a general good agreement among these values. Quantitatively, the average of such differences gives  $\Delta T_{\text{eff}} = T_{\text{eff}}^{\text{spec}} - T_{\text{eff}}^{\text{SED}} = 7 \pm 369$  K. These differences

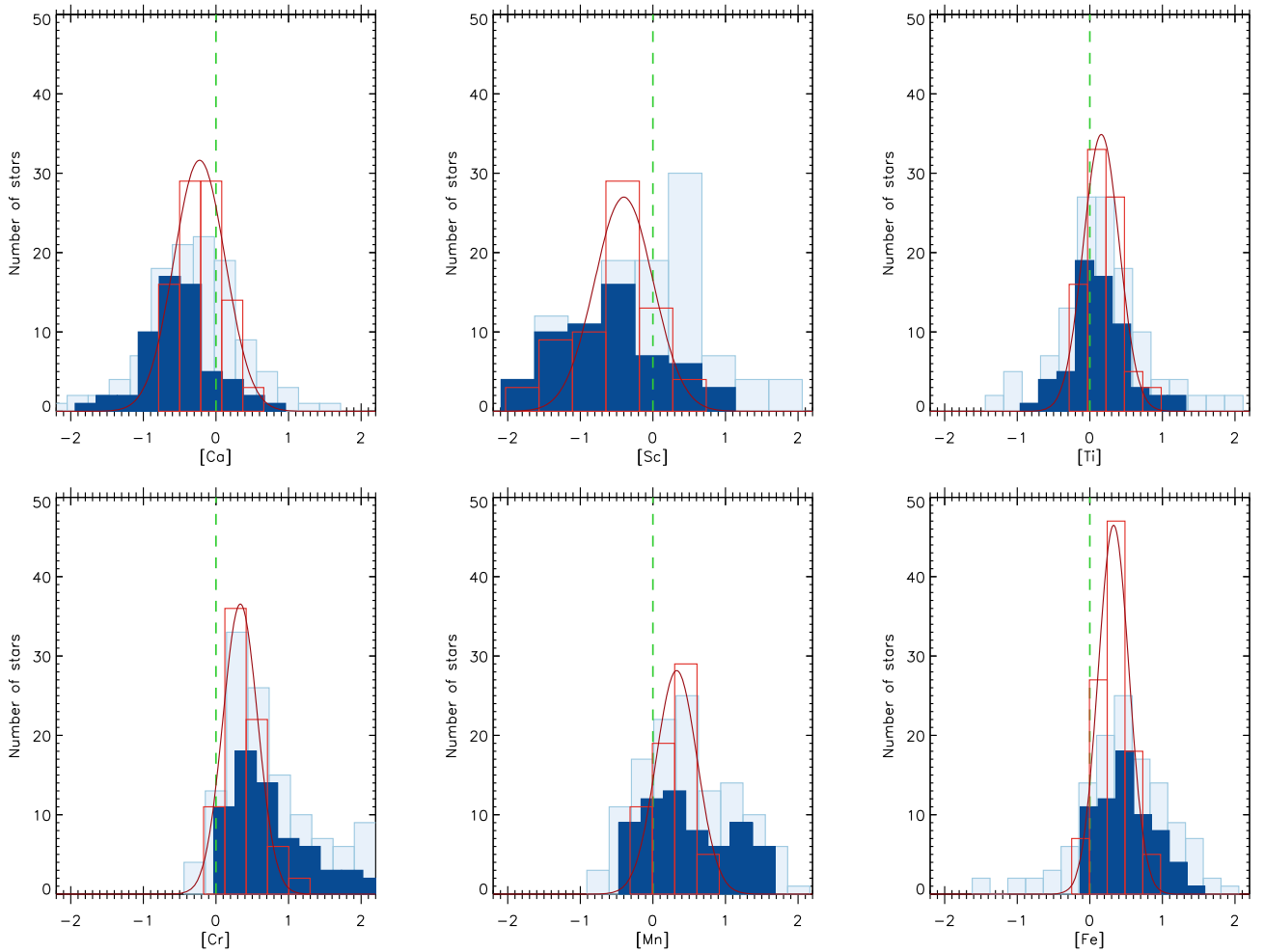


**Figure 2.** Distributions of the abundances of the elements: Ca, Sc, Ti, Cr, Mn, and Fe. Red histogram represents the elements distribution for the Am stars taken from literature with Gaussian fit overimposed. Light blue histograms represent the element distribution for all the suspected CP stars observed by us with Catania Astrophysical Observatory Spectropolarimeter (CAOS) at Osservatorio Astrofisico di Catania (OAC). Dark blue histograms refer to the selected Am stars studied in this paper. The solar abundances taken from Grevesse et al. (2010) are shown as dashed vertical lines.

probably arise because of the blanketing effect that affects the flux distribution over the SED, so we adopted the spectroscopic temperatures for our abundances calculations.

Since the number of stars analysed is quite large, we performed a search for correlations among chemical abundances of elements of Fig. 2 as a function of iron abundance. No significant correlation was found for scandium abundance, being the Spearman’s correlation coefficient  $r \approx 0.0$ , a quite small positive correlation was found between calcium and iron, with correlation coefficient  $r \approx 0.2$ . Significant positive correlations with iron abundance in our sample of Am stars were found for titanium ( $r \approx 0.7$ ), chromium ( $r \approx 0.6$ ), and manganese ( $r \approx 0.7$ ). No evident correlations have been obtained when we plotted abundances as a function of  $v \sin i$ . These results confirm the ones reported by Niemczura et al. (2015).

## 5 POSITION ON THE HR DIAGRAM

An accurate location of the 62 Am stars in the Hertzsprung–Russell (HR) diagram is useful both to investigate possible systematic differences in the region occupied by these objects with respect

to normal F and A stars and also to search for possible pulsating stars.

Historically, it was thought that Am stars did not show pulsations (Breger 1970; Kurtz 1976) due to the gravitational settling of helium from the He II ionization zone where the  $\kappa$ -mechanism drives the pulsation of  $\delta$  Sct stars (Aerts, Christensen-Dalsgaard & Kurtz 2010). By the way, in the last decades some evidence of pulsation in Am stars has been found (Kurtz 1989; Martinez et al. 1999; Henry & Fekel 2005). Recent studies have shown that a large fraction of Am stars pulsate but with lower amplitudes with respect to normal A stars. In this context, Smalley et al. (2011, 2017) by using Super Wide Angle Search for Planets (SuperWASP; Pollacco et al. 2006) light curves, reported about the discovery of a large fraction of Am stars pulsating as  $\delta$  Sct and  $\gamma$  Dor. In particular, Smalley et al. (2017) found that  $\delta$  Sct pulsations in Am stars are mostly confined in the effective temperature range  $6900 \leq T_{\text{eff}} \leq 7600$  K.

To locate our target stars on the HR diagram, we have estimated their  $\log L/L_{\odot}$  values. This task has been accomplished by computing bolometric luminosity scaling the total observed flux to the distance provided by *Gaia* Data Release

**Table 2.** Selected Am star with their distances and luminosity.

Name	$D$ (pc)	$\log L/L_{\odot}$
HD 267	159.537 ± 1.535	0.91 ± 0.10
HD 2887	337.454 ± 5.601	1.49 ± 0.14
HD 6164	568.090 ± 21.695	2.13 ± 0.10
HD 8251	205.848 ± 2.857	1.08 ± 0.20
HD 10088	124.221 ± 0.945	0.81 ± 0.10
HD 13248	166.119 ± 2.027	1.11 ± 0.10
HD 14825	175.254 ± 1.574	1.23 ± 0.14
HD 99620	128.877 ± 0.756	0.93 ± 0.10
HD 108449	147.436 ± 2.081	0.89 ± 0.12
HD 117624	207.964 ± 1.803	1.08 ± 0.10
HD 120049	202.213 ± 2.095	1.12 ± 0.11
HD 124954	112.468 ± 2.796	0.84 ± 0.07
HD 127263	142.192 ± 0.840	0.88 ± 0.18
HD 130771	143.960 ± 2.005	1.10 ± 0.10
HD 132295	249.386 ± 1.643	0.95 ± 0.10
HD 134214	93.179 ± 0.415	0.73 ± 0.12
HD 139939	118.318 ± 5.745	0.94 ± 0.07
HD 143898	120.687 ± 1.086	0.60 ± 0.19
HD 143914	156.785 ± 0.745	0.96 ± 0.10
HD 148980	98.762 ± 0.607	0.82 ± 0.10
HD 149650	114.709 ± 0.948	1.64 ± 0.14
HD 149748	99.203 ± 0.391	0.77 ± 0.10
HD 154226	258.053 ± 1.891	1.45 ± 0.10
HD 155316	131.882 ± 0.583	0.79 ± 0.10
HD 159545	382.599 ± 11.427	1.85 ± 0.10
HD 161660	339.008 ± 10.045	2.43 ± 0.33
HD 163422	229.020 ± 4.604	1.30 ± 0.12
HD 164394	102.510 ± 0.762	0.83 ± 0.05
HD 166016	573.426 ± 16.789	1.73 ± 0.06
HD 166894	314.267 ± 3.122	1.73 ± 0.10
HD 167828	159.490 ± 1.245	1.43 ± 0.10
HD 168796	220.486 ± 2.864	1.40 ± 0.10
HD 169885	101.949 ± 0.381	1.55 ± 0.09
HD 170054	393.433 ± 8.214	2.14 ± 0.14
HD 170563	221.948 ± 5.494	1.28 ± 0.11
HD 171363	146.459 ± 0.651	0.92 ± 0.10
HD 171782	320.440 ± 6.626	1.84 ± 0.10
HD 171914	295.041 ± 4.319	1.71 ± 0.10
HD 176716	141.032 ± 2.764	0.85 ± 0.13
HD 179892	129.567 ± 0.803	0.97 ± 0.12
HD 180347	165.540 ± 0.885	0.88 ± 0.00
HD 184903	365.761 ± 4.779	1.79 ± 0.13
HD 187128	313.659 ± 5.706	1.88 ± 0.10
HD 187959	147.001 ± 0.860	1.11 ± 0.05
HD 188103	333.746 ± 4.987	1.81 ± 0.10
HD 188854	145.010 ± 0.667	1.08 ± 0.10
HD 189574	113.307 ± 0.416	0.80 ± 0.10
HD 190145	153.718 ± 0.711	1.12 ± 0.10
HD 192541	163.276 ± 1.251	1.18 ± 0.17
HD 192662	413.190 ± 7.858	1.33 ± 0.18
HD 198406	218.913 ± 2.665	1.13 ± 0.13
HD 199180	405.551 ± 9.256	1.89 ± 0.13
HD 202431	114.593 ± 2.428	0.94 ± 0.10
HD 207188	304.912 ± 8.033	1.91 ± 0.13
HD 210433	231.047 ± 2.40	1.89 ± 0.05
HD 211643	104.916 ± 0.461	1.08 ± 0.08
HD 211906	233.131 ± 2.692	0.81 ± 0.10
HD 215327	259.777 ± 3.701	1.30 ± 0.13
HD 220668	434.524 ± 11.238	2.28 ± 0.07
HD 223531	144.729 ± 4.617	0.97 ± 0.12
HD 224002	167.938 ± 1.861	1.01 ± 0.10
HD 224657	179.601 ± 3.630	1.25 ± 0.10

**Table 3.** Weighted average abundances derived from our Am stars. Standard deviations have been adopted as weights for single measurements. The last column represents number of stars used in computing the average.

El	[X]	$N_{\text{stars}}$
C	−0.05 ± 0.03	32
O	−0.06 ± 0.03	27
Na	−0.34 ± 0.02	38
Mg	−0.14 ± 0.01	61
Si	0.33 ± 0.01	54
S	0.33 ± 0.01	54
Ca	−0.54 ± 0.02	60
Sc	−0.85 ± 0.02	56
Ti	0.23 ± 0.02	62
V	0.43 ± 0.02	60
Cr	0.82 ± 0.01	62
Mn	0.25 ± 0.01	61
Fe	0.53 ± 0.02	62
Co	0.33 ± 0.03	31
Ni	0.44 ± 0.02	60
Cu	0.06 ± 0.04	29
Zn	0.56 ± 0.03	38
Sr	1.26 ± 0.02	58
Y	1.56 ± 0.02	46
Zr	0.71 ± 0.01	60
Ba	1.69 ± 0.02	41
La	1.65 ± 0.01	46
Ce	1.10 ± 0.01	55
Pr	1.01 ± 0.02	37
Nd	1.40 ± 0.01	56
Sm	1.09 ± 0.01	47
Eu	1.06 ± 0.02	37
Gd	1.53 ± 0.01	56
Dy	1.03 ± 0.02	32

2 (DR2; Gaia Collaboration et al. 2016, 2018) and therefore estimates the bolometric luminosities of the sources in our sample:

$$L(L_{\odot}) = 4\pi D^2 F_{\text{obs}}, \quad (2)$$

where the observed flux has been computed by VOSA tools. These logarithm luminosities have been reported in Table 2, and plotted as a function of the effective temperatures, to build the HR diagram showed in Fig. 7.

Regarding pulsations, in the classification scheme proposed by Grigahcène et al. (2010),  $\delta$  Sct stars show frequencies above 5 d<sup>−1</sup>, while  $\gamma$  Dor lower than 5 d<sup>−1</sup>. An accurate analysis of the power spectrum of these stars should be made in order to ascertain if pulsations occur and then to classify each object according to their pattern. We searched in literature for time-resolved photometry of these targets. Only two objects (HD 180347 and HD 188854) have been found in the *Kepler* archive and only one (HD 6164) in the K2 archive. Most of them, 52 stars, could be observable by *Transiting Exoplanet Survey Satellite (TESS)* in next Cycle 2, so they could be targets of a proposal aimed at understanding the occurrence of pulsations in Am stars.

Therefore, given the lack of data, we decided to proceed as follows: in Fig. 7, we plotted the edges of the  $\delta$  Sct (Breger & Pamyatnykh 1998) and  $\gamma$  Dor (Warner et al. 2003) theoretical instability strips. The locus on the diagram bounded by the blue edge of the  $\gamma$  Dor and the red edge of the  $\delta$  Sct strips is usually occupied by the so-called hybrid stars, i.e. object that show pulsational properties



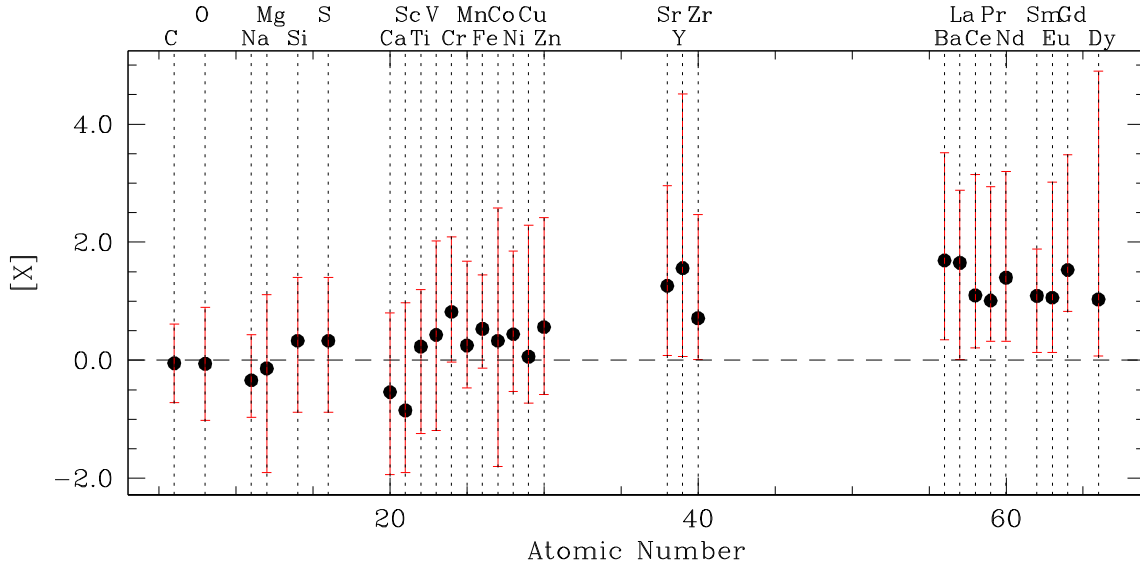


**Figure 3.** Average abundance pattern for our sample of Am stars. Points represent the weighted average abundance plotted versus atomic number, standard deviations have been adopted as weights for single measurements. Bars extend from minimum to maximum abundances derived in our sample.

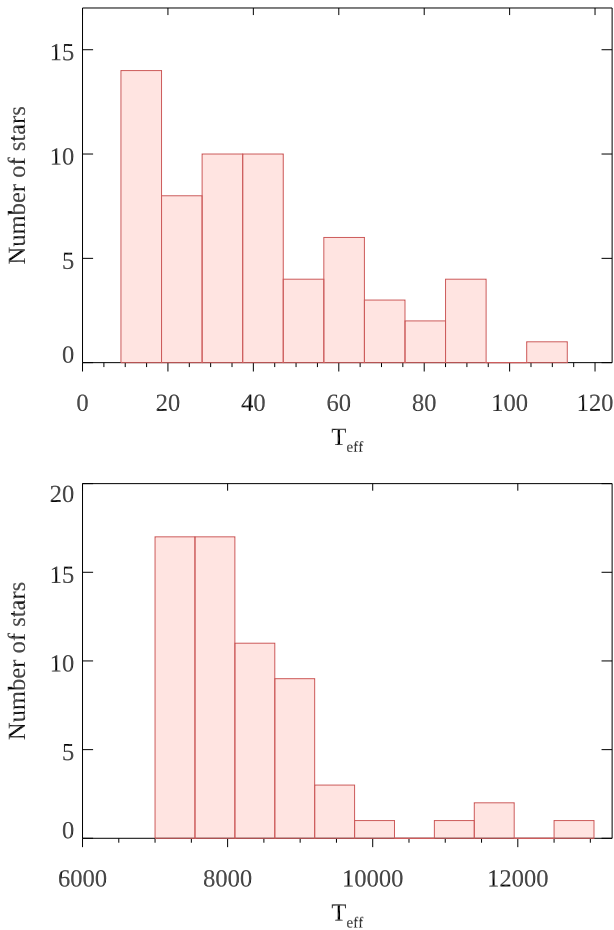


**Figure 4.** Histograms of distribution for rotational velocity (top panel) and effective temperature (bottom panel) derived in this paper for our sample of selected Am stars.

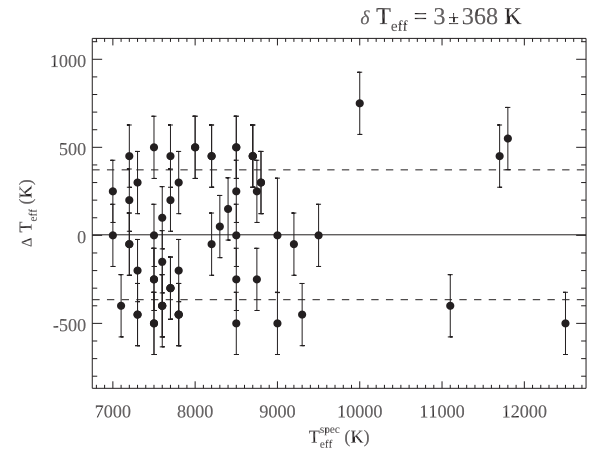


**Figure 5.** Comparison of  $T_{\text{eff}}$  obtained spectroscopically and by SED fitting, in the y-axis  $\Delta T$  represents the difference  $T_{\text{eff}}^{\text{spec}} - T_{\text{eff}}^{\text{SED}}$ . Arithmetic mean and standard deviation are indicated in figure with solid and dashed lines, respectively.

common to both types. Analysing Fig. 7, we defined candidates  $\delta$  Sct stars all the objects that fall within the blue edge of the  $\delta$  Sct instability strip and the blue edge of the  $\gamma$  Dor strip and candidates hybrid stars the ones falling within the blue edge of the  $\gamma$  Dor strip and the red edge of the  $\delta$  Sct strip. We did not find any  $\gamma$  Dor candidate stars. These objects are listed in Table 4, where we report 42 candidates  $\delta$  Sct and only four candidate hybrid stars.

Of course, our classification reflects the choice of the instability strips boundaries. These boundaries depend on many factors, such as metallicity, mixing-length, and convection treatment (Dupret et al. 2004, 2005; Xiong, Deng & Zhang 2015; Xiong et al. 2016). Moreover, thanks to new results coming from space-based data, our understanding of stellar pulsation has evolved quite considerably over the last few decades. In fact, Grigahcène et al. (2010) and

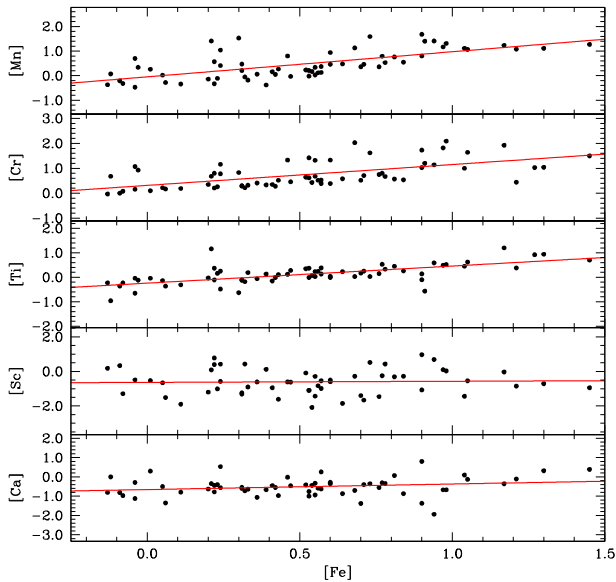


**Figure 6.** Abundances of calcium, scandium, titanium, chromium, and manganese as a function of iron abundance for our Am stars.

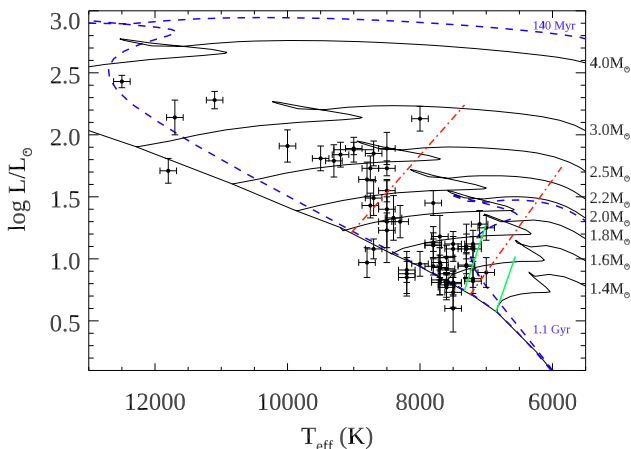


**Figure 7.** HR diagram for the 62 Am stars investigated in this paper. The red dot-dashed lines show the  $\delta$  Sct instability strip by (Breger & Pamyatnykh 1998); the green dash-dot-dot lines show the theoretical edges of the  $\gamma$  Dor instability strip by Warner, Kaye & Guzik (2003). The evolutionary tracks (thin solid lines) for the labelled masses and the zero-age main sequence (ZAMS; thick solid line), and the two isochrones at 140 Myr and 1.1 Gyr are from Girardi et al. (2000) for  $Z = 0.019$  (blue dashed lines).

Uytterhoeven et al. (2011) first found that the *Kepler*  $\gamma$  Dor and  $\delta$  Sct stars and hybrids are not clearly separated into the instability regions formerly established by the theoretical models. Recently, by using *Kepler* data, Balona (2018) showed evidence that the  $\gamma$  Dor variables do not occupy a separate instability strip, but lie entirely within the  $\delta$  Sct instability region. So, an accurate analysis of the frequencies pattern is necessary to determine if and how the stars pulsate.

Regarding the ages of the stars, by using isochrones from Girardi et al. (2000), we concluded that they are in the range between 140 Myr and 1.1 Gyr.

**Table 4.** Candidate pulsating Am stars.

$\delta$ Sct			Hybrids
HD 267	HD 143914	HD 189574	HD 108449
HD 2887	HD 149748	HD 190145	HD 124954
HD 8251	HD 154226	HD 192541	HD 148980
HD 10088	HD 155316	HD 192662	HD 170563
HD 13248	HD 163422	HD 198406	
HD 14825	HD 164394	HD 202431	
HD 99620	HD 167828	HD 211643	
HD 117624	HD 168796	HD 211906	
HD 120049	HD 169885	HD 215327	
HD 127263	HD 171363	HD 223531	
HD 130771	HD 176716	HD 224002	
HD 132295	HD 179892	HD 224657	
HD 134214	HD 180347		
HD 139939	HD 187959		
HD 143898	HD 188854		

## 6 CONCLUSIONS

In this work we classify 62 new Am stars (see Table 2), selected among a sample of 126 suspected CP stars (see Table 1) in Renson & Manfroid (2009), and we present a detailed spectroscopic analysis for each of them. The analysis is based on high-resolution spectra obtained at the 91-cm telescope of the Catania Astrophysical Observatory equipped with the CAOS spectrograph.

For all the stars of our sample, fundamental parameters such as effective temperatures, gravities, rotational and radial velocities, and abundances of chemical elements were determined by using spectral synthesis method. In particular LTE atmospheric models have been computed by ATLAS9 (Kurucz 1993a) and spectral synthesis have been performed by using SYNTHE (Kurucz & Avrett 1981).

By using a set of well-known Am stars collected from literature, we defined an abundance-based criterion that led us to select 62 Am star candidates.

Average abundances show that elements such as silicon, sulfur, and those heavier than titanium are overabundant by a factor ranging from 0.2 to 1.2 than the Sun, while underabundances have been measured not only for calcium and scandium, but also for oxygen and sodium. Solar abundances have been inferred for carbon and magnesium.

We searched for correlation between abundances of calcium, scandium, titanium, chromium, and manganese with iron abundance. While no significant correlation has been found for calcium and scandium, iron-peak elements show positive correlation with iron.

Furthermore, the values of  $T_{\text{eff}}$  derived in this work and distances by *Gaia* have been used to estimate the luminosity of the stars and to place the Am stars on the HR diagram. We used the theoretical instability strips for  $\delta$  Sct (Breger & Pamyatnykh 1998) and  $\gamma$  Dor (Warner et al. 2003) to select a number of candidates pulsating stars, in particular we found 42 stars falling in the  $\delta$  Sct region and only four star candidates to be hybrid pulsators.

By using the isochrones by Girardi et al. (2000) we established a range for the ages of our targets between 140 Myr and 1.1 Gyr.

As a final remark, we refer the reader to a forthcoming paper for the remaining stars of this sample not classified as Am stars. Moreover the observational campaign aimed at observing all the selected uncertain stars of the Renson & Manfroid (2009) catalogue is still ongoing.

## ACKNOWLEDGEMENTS

This study is based on observations made with the Catania Astrophysical Observatory Spectropolarimeter (CAOS) operated by the Catania Astrophysical Observatory.

This publication makes use of VOSA, developed under the Spanish Virtual Observatory project supported from the Spanish MICINN through grant AyA2011-24052.

This research has made use of the SIMBAD data base and VizieR catalogue access tool, operated at CDS, Strasbourg, France.

This work has made use of data from the European Space Agency (ESA) mission *Gaia* (<https://www.cosmos.esa.int/gaia>), processed by the *Gaia* Data Processing and Analysis Consortium (DPAC; <https://www.cosmos.esa.int/web/gaia/dpac/consortium>). Funding for the DPAC has been provided by national institutions, in particular the institutions participating in the *Gaia* Multilateral Agreement.

## REFERENCES

- Abt H. A., 2000, *ApJ*, 544, 933  
 Abt H. A., 2009, *AJ*, 138, 28  
 Aerts C., Christensen-Dalsgaard J., Kurtz D. W., 2010, *Asteroseismology*, Astronomy and Astrophysics Library. Springer-Verlag, Berlin  
 Balona L. A., 2018, *MNRAS*, 479, 183  
 Bayo A., Rodrigo C., Barrado Y Navascués D., Solano E., Gutiérrez R., Morales-Calderón M., Allard F., 2008, *A&A*, 492, 277  
 Breger M., 1970, *ApJ*, 162, 597  
 Breger M., Pamyatnykh A. A., 1998, *A&A*, 332, 958  
 Brown T. M., Latham D. W., Everett M. E., Esquerdo G. A., 2011, *AJ*, 142, 112  
 Castelli F., Hubrig S., 2004, *A&A*, 425, 263  
 Castelli F., Gratton R., Kurucz R. L., 1997, *A&A*, 318, 841 (erratum: 1997, *A&A*, 324, 432)  
 Catanzaro G., Balona L., 2012, *MNRAS*, 421, 1222  
 Catanzaro G., Ripepi V., 2014, *MNRAS*, 441, 1669  
 Catanzaro G., Ripepi V., Bruntt H., 2013, *MNRAS*, 431, 3258  
 Catanzaro G. et al., 2015, *MNRAS*, 451, 184  
 Dupret M.-A., Grigahcène A., Garrido R., Gabriel M., Scuflaire R., 2004, *A&A*, 414, 17  
 Dupret M.-A., Grigahcène A., Garrido R., Gabriel M., Scuflaire R., 2005, *A&A*, 435, 927  
 Gaia Collaboration et al., 2016, *A&A*, 595, A1  
 Gaia Collaboration et al., 2018, *A&A*, 616, A1  
 Gebran M., Monier R., Royer F., Lobel A., Blomme R., 2014, in Mathys G., Griffin E., Kochukhov O., Monier R., Wahlgren G., eds, *Putting A Stars into Context: Evolution, Environment, and Related Stars*. Publishing house ‘Pero’, Moscow, p. 193  
 Girardi L., Bressan A., Bertelli G., Chiosi C., 2000, *A&AS*, 141, 371  
 Grevesse N., Sauval A. J., 1998, *Space Sci. Rev.*, 85, 161  
 Grevesse N., Asplund M., Sauval A. J., Scott P., 2010, *Ap&SS*, 328, 179  
 Grigahcène A. et al., 2010, *ApJ*, 713, L192  
 Henry G. W., Fekel F. C., 2005, *AJ*, 129, 2026  
 Høg E. et al., 2000, *A&A*, 355, L27  
 Kurtz D. W., 1976, *ApJS*, 32, 651  
 Kurtz D. W., 1989, *MNRAS*, 238, 1077  
 Kurucz R. L., 1993a, *ATLAS9 Stellar Atmosphere Programs and 2 km/s grid*. Kurucz CD-ROM No. 13. Smithsonian Astrophysical Observatory, Cambridge, MA  
 Kurucz R. L., 1993b, in Dworetzky M. M., Castelli F., Faraggiana R., eds, *IAU Colloq. 138, ASP Conf. Ser. Vol. 44, Peculiar versus Normal Phenomena in A-type and Related Stars*. Astron. Soc. Pac., San Francisco, p. 87  
 Kurucz R. L., Avrett E. H., 1981, *SAO Special Rep.*, 391  
 Kurucz R. L., Bell B., 1995, *Atomic Line Data*. Kurucz CD-ROM No. 23. Smithsonian Astrophysical Observatory, Cambridge, MA  
 Lampton M., Margon B., Bowyer S., 1976, *ApJ*, 208, 177  
 Leone F. et al., 2016, *AJ*, 151, 116  
 Martínez P. et al., 1999, *MNRAS*, 309, 871  
 Niemczura E. et al., 2015, *MNRAS*, 450, 2764  
 Paunzen E., 2015, *A&A*, 580, A23  
 Pollacco D. L. et al., 2006, *PASP*, 118, 1407  
 Renson P., Manfroid J., 2009, *A&A*, 498, 961  
 Royer F., 2009, in Rozelot J.-P., Neiner C., eds, *Lecture Notes in Physics*, Vol. 765, *The Rotation of Sun and Stars*. Springer-Verlag, Berlin, p. 207  
 Skrutskie M. F. et al., 2006, *AJ*, 131, 1163  
 Smalley B. et al., 2011, *A&A*, 535, A3  
 Smalley B. et al., 2017, *MNRAS*, 465, 2662  
 Uytterhoeven K. et al., 2011, *A&A*, 534, A125  
 Warner P. B., Kaye A. B., Guzik J. A., 2003, *ApJ*, 593, 1049  
 Wright E. L. et al., 2010, *AJ*, 140, 1868  
 Xiong D. R., Deng L., Zhang C., 2015, *MNRAS*, 451, 3354  
 Xiong D. R., Deng L., Zhang C., Wang K., 2016, *MNRAS*, 457, 3163  
 Yüce K., Adelman S. J., 2014, *PASP*, 126, 345

## APPENDIX: SINGLE STAR ABUNDANCES

In this section we report the chemical abundances derived for each single Am star of our sample, as described in Section 3. All the abundances are expressed in terms of the solar one (Grevesse et al. 2010).

**Table A1.** Abundances derived for Am stars. All values are expressed in terms of solar one as given by Grevesse et al. (2010).

	HD 267	HD 2887	HD 6164	HD 8251	HD 10088	HD 13248	HD 14825	HD 99620	HD 108449
C	0.6 ± 0.2	0.3 ± 0.1	-0.4 ± 0.2	0.3 ± 0.1	-0.1 ± 0.2	-0.5 ± 0.1	-	-	0.2 ± 0.2
O	-	0.1 ± 0.2	0.3 ± 0.2	-	-	-	-	-0.1 ± 0.1	-
Na	0.2 ± 0.1	-	-	-0.9 ± 0.4	-0.2 ± 0.1	-0.0 ± 0.2	-	-0.4 ± 0.1	-0.6 ± 0.1
Mg	0.5 ± 0.1	-0.2 ± 0.1	-1.8 ± 0.1	0.4 ± 0.2	0.2 ± 0.1	0.3 ± 0.2	0.5 ± 0.2	0.4 ± 0.1	0.1 ± 0.1
Si	0.5 ± 0.3	0.0 ± 0.2	-0.9 ± 0.2	0.2 ± 0.2	0.1 ± 0.2	0.4 ± 0.1	1.4 ± 0.3	0.5 ± 0.3	0.4 ± 0.1
S	-	1.1 ± 0.1	0.5 ± 0.1	-	-	0.5 ± 0.2	0.3 ± 0.3	-0.5 ± 0.3	0.2 ± 0.1
Ca	0.1 ± 0.1	-0.4 ± 0.2	-1.1 ± 0.2	0.3 ± 0.1	-1.4 ± 0.1	-0.4 ± 0.1	0.3 ± 0.2	-0.6 ± 0.1	-0.8 ± 0.2
Sc	-0.3 ± 0.1	-0.0 ± 0.4	-0.5 ± 0.3	-0.5 ± 0.3	-1.4 ± 0.1	-1.7 ± 0.2	-0.5 ± 0.2	-0.9 ± 0.2	0.2 ± 0.6
Ti	0.4 ± 0.2	1.2 ± 0.1	-0.6 ± 0.1	0.1 ± 0.1	0.2 ± 0.1	0.2 ± 0.1	0.0 ± 0.1	0.2 ± 0.1	-0.2 ± 0.1
V	-0.5 ± 0.2	-	1.0 ± 0.2	-0.8 ± 0.1	0.9 ± 0.2	1.1 ± 0.2	0.8 ± 0.1	0.7 ± 0.1	0.0 ± 0.1
Cr	0.6 ± 0.1	1.9 ± 0.1	2.0 ± 0.2	0.4 ± 0.1	0.5 ± 0.2	0.7 ± 0.2	0.1 ± 0.1	0.3 ± 0.1	0.0 ± 0.1
Mn	0.8 ± 0.1	1.2 ± 0.3	0.7 ± 0.2	0.4 ± 0.1	0.4 ± 0.1	0.5 ± 0.1	0.3 ± 0.1	-0.2 ± 0.1	-0.4 ± 0.1
Fe	0.8 ± 0.1	1.1 ± 0.1	0.0 ± 0.2	0.6 ± 0.2	0.7 ± 0.1	0.7 ± 0.2	0.0 ± 0.1	0.3 ± 0.1	0.0 ± 0.1
Co	-	-	-1.5 ± 0.2	-1.8 ± 0.2	1.1 ± 0.1	1.5 ± 0.1	-	-	0.0 ± 0.1
Ni	0.6 ± 0.2	0.4 ± 0.2	-0.4 ± 0.2	0.4 ± 0.1	0.4 ± 0.1	0.8 ± 0.1	-0.5 ± 0.1	0.2 ± 0.1	0.1 ± 0.2
Cu	-0.1 ± 0.3	-	-	-	-	0.3 ± 0.1	-	-	-0.1 ± 0.3
Zn	1.3 ± 0.1	-0.0 ± 0.2	-	0.5 ± 0.4	0.6 ± 0.1	1.1 ± 0.2	-	-	0.0 ± 0.1
Sr	1.7 ± 0.2	0.9 ± 0.3	-0.7 ± 0.4	1.1 ± 0.1	1.3 ± 0.3	1.4 ± 0.1	1.7 ± 0.1	1.2 ± 0.1	0.6 ± 0.1
Y	1.6 ± 0.1	0.4 ± 0.3	-	1.3 ± 0.1	1.9 ± 0.4	1.7 ± 0.2	-0.3 ± 0.5	0.8 ± 0.1	-0.4 ± 0.1
Zr	0.7 ± 0.2	0.0 ± 0.3	0.4 ± 0.2	1.1 ± 0.1	0.8 ± 0.2	1.4 ± 0.1	0.9 ± 0.1	0.5 ± 0.2	-0.5 ± 0.1
Ba	0.8 ± 0.1	-0.4 ± 0.1	-1.2 ± 0.1	1.6 ± 0.2	2.1 ± 0.2	2.5 ± 0.1	-0.3 ± 0.6	1.9 ± 0.2	0.5 ± 0.1
La	1.9 ± 0.1	1.5 ± 0.4	0.9 ± 0.1	1.0 ± 0.2	2.2 ± 0.2	1.8 ± 0.2	-	1.2 ± 0.2	1.0 ± 0.1
Ce	0.4 ± 0.2	-	0.5 ± 0.1	0.6 ± 0.1	0.9 ± 0.1	1.4 ± 0.1	0.3 ± 0.2	0.7 ± 0.1	-
Pr	1.8 ± 0.1	-	1.0 ± 0.1	-	-	1.2 ± 0.1	2.0 ± 0.4	0.7 ± 0.1	0.8 ± 0.2
Nd	1.7 ± 0.1	1.1 ± 0.1	1.1 ± 0.2	0.6 ± 0.1	0.7 ± 0.1	1.0 ± 0.2	-	1.0 ± 0.2	0.3 ± 0.1
Sm	-0.0 ± 0.1	-	1.4 ± 0.1	-	0.5 ± 0.2	1.1 ± 0.1	1.2 ± 0.1	0.9 ± 0.1	0.2 ± 0.1
Eu	-	1.3 ± 0.1	0.9 ± 0.1	0.6 ± 0.2	0.5 ± 0.2	1.6 ± 0.1	1.2 ± 0.1	-	-
Gd	1.0 ± 0.2	2.3 ± 0.1	1.3 ± 0.1	1.1 ± 0.2	1.6 ± 0.5	1.4 ± 0.1	1.6 ± 0.2	1.4 ± 0.3	0.8 ± 0.1
Dy	0.9 ± 0.1	1.8 ± 0.1	-	-	-	1.1 ± 0.1	1.9 ± 0.1	1.1 ± 0.5	-

	HD 117624	HD 120049	HD 124954	HD 127263	HD 130771	HD 132295	HD 134214	HD 139939	HD 143898
C	-0.6 ± 0.1	-	-	-	0.0 ± 0.2	0.3 ± 0.2	0.0 ± 0.1	-	-
O	-	-	-	-0.6 ± 0.1	0.5 ± 0.1	-	-0.9 ± 0.1	-0.2 ± 0.2	-0.9 ± 0.1
Na	-0.3 ± 0.1	-0.4 ± 0.1	-0.7 ± 0.1	0.1 ± 0.3	-0.5 ± 0.1	-0.3 ± 0.2	-0.6 ± 0.1	-	-0.2 ± 0.1
Mg	0.2 ± 0.1	0.1 ± 0.2	0.0 ± 0.1	0.3 ± 0.1	0.2 ± 0.1	0.3 ± 0.1	0.4 ± 0.1	0.1 ± 0.2	0.3 ± 0.2
Si	0.3 ± 0.1	0.4 ± 0.1	0.1 ± 0.1	-0.2 ± 0.1	0.2 ± 0.2	0.4 ± 0.3	0.4 ± 0.2	0.2 ± 0.2	0.1 ± 0.2
S	0.6 ± 0.2	-	-0.5 ± 0.3	0.1 ± 0.1	0.6 ± 0.1	-	0.3 ± 0.2	-0.3 ± 0.1	0.4 ± 0.1
Ca	-0.6 ± 0.1	-0.8 ± 0.1	-1.3 ± 0.1	-0.3 ± 0.2	-0.6 ± 0.1	-0.7 ± 0.2	0.5 ± 0.1	-0.6 ± 0.1	-0.6 ± 0.1
Sc	-1.5 ± 0.2	-1.9 ± 0.1	-1.5 ± 0.2	-0.2 ± 0.6	-1.3 ± 0.2	0.4 ± 0.3	-0.6 ± 0.5	-1.2 ± 0.2	-0.8 ± 0.2
Ti	0.1 ± 0.2	-0.3 ± 0.2	-0.4 ± 0.2	0.5 ± 0.1	-0.1 ± 0.2	-0.2 ± 0.2	0.2 ± 0.1	0.0 ± 0.1	0.2 ± 0.2
V	1.0 ± 0.1	-1.0 ± 0.1	-1.2 ± 0.1	-0.5 ± 0.2	0.5 ± 0.2	0.5 ± 0.1	1.2 ± 0.1	-0.9 ± 0.2	0.8 ± 0.1
Cr	0.7 ± 0.2	0.2 ± 0.2	0.2 ± 0.1	0.8 ± 0.2	0.3 ± 0.2	0.2 ± 0.2	0.8 ± 0.1	0.3 ± 0.1	0.5 ± 0.1
Mn	0.4 ± 0.1	-0.3 ± 0.1	-0.3 ± 0.1	0.8 ± 0.2	0.5 ± 0.2	0.0 ± 0.1	1.0 ± 0.2	-0.1 ± 0.1	0.1 ± 0.1
Fe	0.8 ± 0.2	0.1 ± 0.1	0.1 ± 0.2	0.8 ± 0.1	0.3 ± 0.1	0.3 ± 0.1	0.2 ± 0.1	0.2 ± 0.1	0.6 ± 0.2
Co	-	0.7 ± 0.2	0.6 ± 0.1	-	0.8 ± 0.1	0.8 ± 0.1	1.7 ± 0.2	-	0.7 ± 0.1
Ni	0.8 ± 0.1	0.4 ± 0.1	0.2 ± 0.2	0.8 ± 0.1	0.4 ± 0.2	0.2 ± 0.2	-0.1 ± 0.1	0.4 ± 0.2	0.5 ± 0.2
Cu	0.4 ± 0.1	1.6 ± 0.3	0.0 ± 0.2	0.7 ± 0.1	-0.6 ± 0.1	-0.7 ± 0.1	-0.6 ± 0.5	0.1 ± 0.4	-0.1 ± 0.4
Zn	1.5 ± 0.5	0.2 ± 0.4	0.3 ± 0.4	1.1 ± 0.1	0.6 ± 0.3	0.2 ± 0.1	0.3 ± 0.1	-	0.7 ± 0.3
Sr	1.2 ± 0.1	1.1 ± 0.6	1.0 ± 0.3	1.5 ± 0.1	0.6 ± 0.1	1.1 ± 1.1	1.4 ± 0.1	1.3 ± 0.2	1.1 ± 0.1
Y	1.7 ± 0.1	0.4 ± 0.2	0.2 ± 0.2	1.3 ± 0.2	1.0 ± 0.1	0.9 ± 0.2	0.9 ± 0.2	0.3 ± 0.2	1.5 ± 0.1
Zr	1.2 ± 0.1	0.8 ± 0.2	0.1 ± 0.1	0.0 ± 0.1	0.8 ± 0.1	0.7 ± 0.2	1.2 ± 0.2	0.5 ± 0.2	0.1 ± 0.1
Ba	2.5 ± 0.3	1.1 ± 0.1	1.6 ± 0.1	2.7 ± 0.2	1.9 ± 0.1	1.6 ± 0.1	1.3 ± 0.1	1.6 ± 0.2	2.2 ± 0.2
La	1.6 ± 0.1	1.5 ± 0.2	1.0 ± 0.2	1.7 ± 0.1	1.1 ± 0.1	1.7 ± 0.2	2.2 ± 0.2	1.9 ± 0.1	1.4 ± 0.2
Ce	1.3 ± 0.2	0.3 ± 0.2	0.6 ± 0.1	1.6 ± 0.1	0.8 ± 0.1	0.4 ± 0.1	1.5 ± 0.1	0.7 ± 0.1	1.1 ± 0.2
Pr	1.1 ± 0.1	0.3 ± 0.2	0.7 ± 0.1	1.2 ± 0.1	-	0.7 ± 0.1	0.9 ± 0.1	1.1 ± 0.2	0.5 ± 0.1
Nd	0.9 ± 0.1	1.0 ± 0.1	0.5 ± 0.2	1.1 ± 0.2	0.7 ± 0.2	0.8 ± 0.2	1.5 ± 0.2	0.8 ± 0.1	0.8 ± 0.1
Sm	1.0 ± 0.1	0.1 ± 0.1	0.6 ± 0.4	1.1 ± 0.1	0.6 ± 0.2	0.4 ± 0.1	1.8 ± 0.2	0.8 ± 0.2	0.8 ± 0.2
Eu	1.6 ± 0.1	0.4 ± 0.4	0.1 ± 0.2	1.3 ± 0.1	0.4 ± 0.1	0.4 ± 0.2	1.6 ± 0.1	0.7 ± 0.2	0.8 ± 0.2
Gd	1.2 ± 0.1	1.2 ± 0.0	1.0 ± 0.1	1.2 ± 0.3	1.3 ± 0.1	1.2 ± 0.1	1.9 ± 0.1	1.2 ± 0.1	0.8 ± 0.3
Dy	0.8 ± 0.1	-	0.1 ± 0.1	1.7 ± 0.2	1.1 ± 0.1	-	1.2 ± 0.1	0.1 ± 0.1	0.9 ± 0.1

Table A1 – continued

	HD 143914	HD 148980	HD 149650	HD 149748	HD 154226	HD 155316	HD 159545	HD 161660	HD 163422
C	–	–	–	0.2 ± 0.2	0.0 ± 0.2	–0.2 ± 0.1	–	–	–
O	–	–	–	–	–0.3 ± 0.3	–	0.5 ± 0.2	–	–
Na	–	–0.5 ± 0.1	–	–1.0 ± 0.1	–0.5 ± 0.4	–	–	–	–
Mg	0.2 ± 0.2	0.2 ± 0.1	0.4 ± 0.1	0.3 ± 0.2	0.3 ± 0.2	0.3 ± 0.2	–	–1.2 ± 0.2	–
Si	0.4 ± 0.1	–	–	0.4 ± 0.1	0.4 ± 0.2	0.2 ± 0.2	0.7 ± 0.1	–0.1 ± 0.2	–
S	–0.7 ± 0.4	–	1.0 ± 0.1	0.2 ± 0.1	1.4 ± 0.4	1.1 ± 0.1	0.9 ± 0.1	–0.2 ± 0.1	1.2 ± 0.1
Ca	–0.5 ± 0.2	–0.8 ± 0.1	–0.3 ± 0.1	–0.9 ± 0.1	–0.6 ± 0.1	–0.4 ± 0.1	–0.8 ± 0.1	–0.3 ± 0.4	–0.6 ± 0.1
Sc	–0.6 ± 0.4	0.3 ± 0.4	–	–0.3 ± 0.4	–1.0 ± 0.3	–1.0 ± 0.3	0.8 ± 0.2	0.1 ± 0.2	0.4 ± 0.2
Ti	0.3 ± 0.1	–0.4 ± 0.1	0.0 ± 0.1	0.3 ± 0.2	0.4 ± 0.2	–0.1 ± 0.2	0.4 ± 0.2	1.2 ± 0.1	–0.5 ± 0.2
V	0.7 ± 0.2	–1.2 ± 0.1	–	–0.6 ± 0.1	1.1 ± 0.1	0.6 ± 0.2	0.6 ± 0.1	–	1.3 ± 0.2
Cr	0.5 ± 0.2	0.0 ± 0.1	0.2 ± 0.1	0.5 ± 0.1	0.5 ± 0.2	0.3 ± 0.2	0.8 ± 0.1	0.7 ± 0.1	1.2 ± 0.1
Mn	0.0 ± 0.1	–0.2 ± 0.1	–0.5 ± 0.3	0.5 ± 0.1	0.1 ± 0.1	0.2 ± 0.2	0.6 ± 0.1	1.4 ± 0.2	0.4 ± 0.1
Fe	0.5 ± 0.1	–0.1 ± 0.2	–0.1 ± 0.1	0.8 ± 0.2	0.6 ± 0.2	0.4 ± 0.2	0.2 ± 0.1	0.2 ± 0.1	0.2 ± 0.2
Co	–	0.2 ± 0.1	–	–	–	–	0.0 ± 0.1	1.7 ± 0.2	–1.1 ± 0.2
Ni	0.2 ± 0.2	0.1 ± 0.2	–	0.6 ± 0.1	0.4 ± 0.2	0.4 ± 0.2	0.6 ± 0.2	0.6 ± 0.1	0.4 ± 0.1
Cu	–	–0.6 ± 0.1	–	–	–	–	–	–	–
Zn	0.8 ± 0.1	–	–	0.7 ± 0.4	0.6 ± 0.1	0.6 ± 0.1	–	–	–
Sr	1.4 ± 0.3	1.0 ± 0.4	–	1.2 ± 0.1	1.7 ± 0.4	1.5 ± 0.3	0.3 ± 0.5	0.8 ± 0.4	2.0 ± 0.5
Y	1.0 ± 0.1	0.8 ± 0.1	0.8 ± 0.3	1.3 ± 0.1	1.8 ± 0.1	1.3 ± 0.3	–0.5 ± 0.4	–	–
Zr	0.5 ± 0.2	0.1 ± 0.1	1.2 ± 0.1	0.6 ± 0.1	1.3 ± 0.2	0.4 ± 0.2	0.7 ± 0.1	2.3 ± 0.1	0.1 ± 0.4
Ba	1.7 ± 0.2	0.4 ± 0.1	–	1.9 ± 0.1	2.2 ± 0.2	2.0 ± 0.1	–	2.9 ± 0.1	–
La	2.1 ± 0.1	1.6 ± 0.2	–	1.9 ± 0.1	1.3 ± 0.1	1.5 ± 0.1	1.2 ± 0.1	–	2.1 ± 0.5
Ce	0.8 ± 0.1	0.2 ± 0.1	0.4 ± 0.2	0.5 ± 0.1	1.0 ± 0.1	0.5 ± 0.1	1.3 ± 0.1	–	0.4 ± 0.6
Pr	1.7 ± 0.2	0.6 ± 0.1	–	–	–	–	1.6 ± 0.1	–	–
Nd	1.1 ± 0.1	0.8 ± 0.1	–	0.8 ± 0.1	1.4 ± 0.1	0.7 ± 0.2	1.8 ± 0.2	–	0.8 ± 0.2
Sm	0.8 ± 0.1	–	–	0.5 ± 0.1	0.6 ± 0.1	0.5 ± 0.2	1.8 ± 0.1	–	1.4 ± 0.1
Eu	–	–	–	0.5 ± 0.3	1.3 ± 0.2	–	–	–	–
Gd	1.5 ± 0.2	1.3 ± 0.2	1.8 ± 0.4	1.5 ± 0.1	1.2 ± 0.3	1.3 ± 0.2	2.4 ± 0.1	–	1.7 ± 0.2
Dy	–	–	1.1 ± 0.1	–	1.3 ± 0.3	–	2.4 ± 0.2	–	0.8 ± 0.1
	HD 164394	HD 166016	HD 166894	HD 167828	HD 168796	HD 169885	HD 170054	HD 170563	HD 171363
C	–	–	–	–0.2 ± 0.2	–0.6 ± 0.2	0.4 ± 0.2	–	–	–
O	–	–	–	–0.4 ± 0.1	–0.1 ± 0.1	–0.1 ± 0.2	–	0.9 ± 0.2	–
Na	–0.3 ± 0.1	–	–0.4 ± 0.2	–	–	–	–	–	–0.4 ± 0.3
Mg	0.5 ± 0.1	0.1 ± 0.1	–0.3 ± 0.1	0.0 ± 0.1	–0.1 ± 0.1	1.1 ± 0.2	0.1 ± 0.3	0.3 ± 0.3	0.0 ± 0.1
Si	–	0.6 ± 0.1	0.4 ± 0.1	–0.2 ± 0.2	–0.4 ± 0.1	0.9 ± 0.1	0.4 ± 0.1	0.8 ± 0.2	0.2 ± 0.1
S	0.1 ± 0.4	–0.8 ± 0.2	–0.5 ± 0.3	1.0 ± 0.1	0.5 ± 0.1	–	0.8 ± 0.3	–	–
Ca	–1.0 ± 0.1	–	–0.3 ± 0.1	–0.7 ± 0.1	–0.7 ± 0.1	0.3 ± 0.2	–	–0.5 ± 0.2	–1.0 ± 0.1
Sc	–1.3 ± 0.2	–	–1.4 ± 0.2	0.0 ± 0.4	0.1 ± 0.3	–0.7 ± 0.3	–	–	–1.1 ± 0.2
Ti	–0.2 ± 0.2	–0.1 ± 0.1	0.2 ± 0.1	0.5 ± 0.1	0.5 ± 0.1	0.9 ± 0.2	–0.6 ± 0.2	0.0 ± 0.1	0.0 ± 0.1
V	–0.9 ± 0.2	0.5 ± 0.1	–0.3 ± 0.1	0.6 ± 0.1	1.3 ± 0.2	–0.4 ± 0.2	2.0 ± 0.1	0.2 ± 0.1	0.7 ± 0.2
Cr	0.1 ± 0.1	0.9 ± 0.1	1.3 ± 0.1	2.1 ± 0.2	1.8 ± 0.2	1.0 ± 0.1	1.2 ± 0.1	0.3 ± 0.2	0.6 ± 0.1
Mn	–0.3 ± 0.1	0.3 ± 0.1	0.0 ± 0.2	1.3 ± 0.1	1.2 ± 0.2	1.1 ± 0.2	1.4 ± 0.1	0.0 ± 0.2	0.2 ± 0.1
Fe	–0.1 ± 0.1	0.0 ± 0.2	0.5 ± 0.1	1.0 ± 0.1	1.0 ± 0.2	1.3 ± 0.1	0.9 ± 0.2	0.4 ± 0.2	0.5 ± 0.2
Co	–	–	–	–0.3 ± 0.2	0.7 ± 0.1	–	–	–	0.6 ± 0.1
Ni	0.1 ± 0.2	–0.5 ± 0.1	0.0 ± 0.2	0.3 ± 0.1	0.0 ± 0.2	1.0 ± 0.1	1.6 ± 0.1	0.1 ± 0.2	0.6 ± 0.2
Cu	0.1 ± 0.4	–	–	–	–	–	–	–	0.0 ± 0.1
Zn	–	–	–	0.8 ± 0.1	–0.6 ± 0.4	1.4 ± 0.4	–	–	0.9 ± 0.1
Sr	0.8 ± 0.2	1.6 ± 0.4	0.7 ± 0.4	2.7 ± 0.3	1.4 ± 0.3	2.5 ± 0.2	0.9 ± 0.4	0.1 ± 0.4	1.3 ± 0.1
Y	–0.2 ± 0.3	–	–	0.5 ± 0.1	1.7 ± 0.1	1.6 ± 0.1	–	–0.3 ± 0.2	1.3 ± 0.3
Zr	0.0 ± 0.1	1.4 ± 0.3	0.3 ± 0.2	0.9 ± 0.1	0.9 ± 0.1	1.2 ± 0.1	2.5 ± 0.2	0.3 ± 0.1	0.6 ± 0.2
Ba	1.5 ± 0.1	–	–0.14 ± 0.2	–0.7 ± 0.1	–0.7 ± 0.1	2.3 ± 0.1	–	–0.2 ± 0.1	2.1 ± 0.2
La	0.5 ± 0.1	2.1 ± 0.2	2.0 ± 0.4	1.7 ± 0.1	1.1 ± 0.1	2.9 ± 0.2	–	–	1.2 ± 0.2
Ce	0.4 ± 0.2	1.0 ± 0.2	–	1.9 ± 0.2	1.3 ± 0.2	1.4 ± 0.1	–	0.3 ± 0.1	1.2 ± 0.1
Pr	1.4 ± 0.1	–	–	0.7 ± 0.3	1.2 ± 0.2	–	–	–	1.0 ± 0.2
Nd	0.7 ± 0.2	1.7 ± 0.1	0.6 ± 0.2	1.5 ± 0.1	1.5 ± 0.2	1.9 ± 0.1	–	0.8 ± 0.1	0.9 ± 0.2
Sm	0.3 ± 0.1	0.7 ± 0.5	1.8 ± 0.1	1.6 ± 0.1	1.8 ± 0.1	–	–	0.9 ± 0.2	1.3 ± 0.2
Eu	1.2 ± 0.5	–	1.1 ± 0.2	2.1 ± 0.1	2.4 ± 0.2	0.9 ± 0.2	–	–	1.3 ± 0.1
Gd	1.3 ± 0.1	1.5 ± 0.1	1.6 ± 0.1	2.0 ± 0.1	2.1 ± 0.1	2.2 ± 0.1	–	0.9 ± 0.1	1.0 ± 0.1
Dy	0.4 ± 0.2	–	–	–	–	–	–	1.1 ± 0.2	–



Table A1 – *continued*

	HD 171782	HD 171914	HD 176716	HD 179892	HD 180347	HD 184903	HD 187128	HD 187959	HD 188103
C	–	–	0.6 ± 0.1	0.3 ± 0.2	–	0.4 ± 0.1	–	–	–
O	–1.0 ± 0.1	–	–	–	–0.2 ± 0.1	–0.3 ± 0.1	0.1 ± 0.1	–	–
Na	–	–	0.4 ± 0.2	0.1 ± 0.1	–0.9 ± 0.3	–	–	0.0 ± 0.1	0.1 ± 0.1
Mg	–1.1 ± 0.1	–1.5 ± 0.1	0.5 ± 0.1	0.6 ± 0.1	0.1 ± 0.1	–0.9 ± 0.1	–1.7 ± 0.2	–0.4 ± 0.2	–2.1 ± 0.1
Si	0.8 ± 0.1	0.7 ± 0.2	0.3 ± 0.1	0.4 ± 0.1	0.1 ± 0.1	–	0.3 ± 0.1	0.5 ± 0.3	0.5 ± 0.1
S	0.6 ± 0.1	0.2 ± 0.1	1.1 ± 0.1	–1.3 ± 0.5	–0.4 ± 0.1	0.5 ± 0.1	1.1 ± 0.1	0.5 ± 0.1	1.1 ± 0.1
Ca	–0.3 ± 0.3	–	–0.1 ± 0.2	–0.4 ± 0.1	–1.0 ± 0.2	0.0 ± 0.1	–0.4 ± 0.1	–0.5 ± 0.1	–1.4 ± 0.2
Sc	–0.5 ± 0.2	–	–0.8 ± 0.1	0.4 ± 0.3	–1.6 ± 0.2	–0.6 ± 0.2	0.5 ± 0.4	–0.7 ± 0.4	1.0 ± 0.2
Ti	0.0 ± 0.2	0.9 ± 0.1	0.4 ± 0.2	–0.1 ± 0.2	0.1 ± 0.2	0.1 ± 0.2	0.0 ± 0.2	–0.1 ± 0.2	0.1 ± 0.2
V	0.8 ± 0.1	–0.2 ± 0.1	–0.5 ± 0.2	0.4 ± 0.2	0.7 ± 0.2	1.6 ± 0.2	1.7 ± 0.1	–0.7 ± 0.1	1.2 ± 0.1
Cr	1.3 ± 0.1	1.0 ± 0.1	0.4 ± 0.1	0.2 ± 0.2	0.5 ± 0.2	1.3 ± 0.2	1.6 ± 0.1	0.2 ± 0.1	1.0 ± 0.1
Mn	0.9 ± 0.2	–	1.1 ± 0.1	–0.3 ± 0.4	0.3 ± 0.2	0.8 ± 0.1	1.6 ± 0.2	0.0 ± 0.2	1.7 ± 0.2
Fe	0.6 ± 0.2	1.3 ± 0.2	1.2 ± 0.2	0.2 ± 0.1	0.4 ± 0.1	0.5 ± 0.2	0.7 ± 0.1	0.0 ± 0.1	0.9 ± 0.2
Co	–	–	–	1.8 ± 0.4	0.6 ± 0.2	1.5 ± 0.2	–	–	–
Ni	1.1 ± 0.1	0.9 ± 0.1	0.8 ± 0.1	0.3 ± 0.1	0.5 ± 0.1	0.8 ± 0.1	0.4 ± 0.1	0.4 ± 0.2	–0.2 ± 0.2
Cu	–	–	–	–0.6 ± 0.4	0.1 ± 0.5	–0.7 ± 0.5	–	0.9 ± 0.3	0.9 ± 0.1
Zn	–	–	1.1 ± 0.1	–	0.9 ± 0.1	–	–	0.8 ± 0.3	–
Sr	0.1 ± 0.3	0.1 ± 0.4	1.1 ± 0.4	1.2 ± 0.4	1.2 ± 0.1	1.2 ± 0.5	2.0 ± 0.3	–0.1 ± 0.5	3.0 ± 0.1
Y	–0.4 ± 0.1	1.3 ± 0.1	1.9 ± 0.1	1.3 ± 0.3	1.4 ± 0.1	2.2 ± 0.1	–	0.1 ± 0.3	0.5 ± 0.4
Zr	1.1 ± 0.1	1.4 ± 0.2	1.1 ± 0.2	0.1 ± 0.2	0.6 ± 0.1	0.8 ± 0.1	1.5 ± 0.2	0.2 ± 0.2	1.3 ± 0.1
Ba	–	–	1.7 ± 0.1	1.6 ± 0.2	2.2 ± 0.2	–	–	0.8 ± 0.1	–
La	–	–	1.2 ± 0.1	1.2 ± 0.1	1.3 ± 0.1	–	2.2 ± 0.1	0.0 ± 0.1	–
Ce	1.8 ± 0.2	–	1.1 ± 0.1	0.6 ± 0.1	1.3 ± 0.1	–	2.6 ± 0.1	0.8 ± 0.1	2.2 ± 0.1
Pr	2.1 ± 0.2	–	1.0 ± 0.1	1.3 ± 0.2	0.8 ± 0.1	–	2.8 ± 0.1	1.2 ± 0.2	–
Nd	2.0 ± 0.1	3.2 ± 0.1	1.6 ± 0.2	0.8 ± 0.1	0.6 ± 0.1	–	1.9 ± 0.2	1.2 ± 0.1	2.0 ± 0.1
Sm	1.7 ± 0.1	–	1.6 ± 0.1	0.7 ± 0.1	1.1 ± 0.2	–	1.9 ± 0.2	0.7 ± 0.1	–
Eu	–	–	1.9 ± 0.1	0.4 ± 0.1	1.1 ± 0.1	–	–	–	–
Gd	2.2 ± 0.1	–	3.4 ± 0.1	1.7 ± 0.1	1.2 ± 0.1	–	2.6 ± 0.2	1.3 ± 0.2	–
Dy	2.3 ± 0.1	–	–	–	–	–	2.1 ± 0.2	–	4.6 ± 0.2
	HD 188854	HD 189574	HD 190145	HD 192541	HD 192662	HD 198406	HD 199180	HD 202431	HD 207188
C	–0.7 ± 0.1	–	–0.1 ± 0.2	0.5 ± 0.1	–	0.0 ± 0.1	–0.4 ± 0.1	–	0.4 ± 0.1
O	–0.5 ± 0.3	–	–0.2 ± 0.2	–	–0.6 ± 0.1	–	–0.3 ± 0.2	–0.3 ± 0.2	–
Na	–0.4 ± 0.1	–0.5 ± 0.2	–0.3 ± 0.3	–0.1 ± 0.1	–	–	0.3 ± 0.1	–0.5 ± 0.1	–0.6 ± 0.1
Mg	0.3 ± 0.1	0.0 ± 0.2	0.3 ± 0.1	0.3 ± 0.2	–0.8 ± 0.1	0.3 ± 0.2	–0.9 ± 0.1	0.1 ± 0.1	–1.2 ± 0.1
Si	0.1 ± 0.1	0.2 ± 0.1	0.2 ± 0.1	0.4 ± 0.1	0.0 ± 0.1	–	0.1 ± 0.2	0.1 ± 0.1	0.0 ± 0.2
S	0.5 ± 0.2	–	–0.1 ± 0.1	–	0.8 ± 0.1	0.1 ± 0.4	0.7 ± 0.1	0.3 ± 0.1	1.1 ± 0.1
Ca	–0.4 ± 0.2	–1.1 ± 0.1	–0.4 ± 0.1	–0.4 ± 0.1	–0.8 ± 0.2	–0.4 ± 0.2	–0.7 ± 0.1	–0.9 ± 0.2	–1.9 ± 0.1
Sc	–2.1 ± 0.2	–0.6 ± 0.2	–0.1 ± 0.2	–0.6 ± 0.1	–1.1 ± 0.2	–1.0 ± 0.2	–0.3 ± 0.3	–0.3 ± 0.3	0.7 ± 0.4
Ti	0.1 ± 0.2	–0.1 ± 0.2	0.3 ± 0.1	0.0 ± 0.1	0.4 ± 0.1	0.2 ± 0.1	0.0 ± 0.1	0.0 ± 0.2	0.6 ± 0.2
V	0.7 ± 0.1	0.6 ± 0.1	1.0 ± 0.2	0.8 ± 0.1	0.0 ± 0.2	–1.0 ± 0.1	1.2 ± 0.2	0.6 ± 0.2	–0.3 ± 0.1
Cr	0.4 ± 0.1	0.4 ± 0.2	0.6 ± 0.2	0.4 ± 0.1	1.4 ± 0.2	0.3 ± 0.1	2.0 ± 0.1	0.7 ± 0.1	1.1 ± 0.1
Mn	0.2 ± 0.1	0.1 ± 0.2	0.2 ± 0.1	0.5 ± 0.1	0.0 ± 0.1	–0.1 ± 0.2	1.1 ± 0.1	0.3 ± 0.2	1.4 ± 0.3
Fe	0.5 ± 0.2	0.4 ± 0.2	0.5 ± 0.2	0.6 ± 0.2	0.5 ± 0.1	0.2 ± 0.2	0.7 ± 0.1	0.5 ± 0.2	0.9 ± 0.2
Co	0.7 ± 0.1	0.9 ± 0.1	0.7 ± 0.2	–0.1 ± 0.2	–	–	0.1 ± 0.12	0.5 ± 0.2	2.6 ± 0.1
Ni	0.5 ± 0.1	0.4 ± 0.1	0.5 ± 0.1	0.4 ± 0.2	–	0.3 ± 0.1	–0.1 ± 0.1	0.6 ± 0.2	1.1 ± 0.2
Cu	0.1 ± 0.2	0.0 ± 0.1	0.2 ± 0.1	–	–	–0.7 ± 0.4	–	0.2 ± 0.2	2.3 ± 0.1
Zn	1.2 ± 0.3	0.2 ± 0.1	0.9 ± 0.1	0.6 ± 0.3	–	0.9 ± 0.1	0.5 ± 0.4	1.1 ± 0.3	–
Sr	1.2 ± 0.1	1.2 ± 0.2	1.4 ± 0.1	1.2 ± 0.3	2.2 ± 0.4	1.6 ± 0.2	0.1 ± 0.4	1.2 ± 0.1	–
Y	1.9 ± 0.1	0.9 ± 0.1	1.9 ± 0.1	0.6 ± 0.1	4.5 ± 0.4	1.6 ± 0.1	–	1.5 ± 0.1	2.3 ± 0.3
Zr	1.6 ± 0.2	0.0 ± 0.1	0.9 ± 0.1	0.9 ± 0.2	0.5 ± 0.1	0.2 ± 0.2	0.4 ± 0.2	0.5 ± 0.2	1.7 ± 0.1
Ba	2.3 ± 0.1	1.9 ± 0.1	2.5 ± 0.1	1.9 ± 0.1	–	1.6 ± 0.3	–0.5 ± 0.1	2.1 ± 0.1	–
La	1.5 ± 0.2	1.3 ± 0.2	2.1 ± 0.2	1.6 ± 0.2	–	2.1 ± 0.1	1.5 ± 0.1	1.2 ± 0.1	–
Ce	1.3 ± 0.2	0.8 ± 0.1	1.5 ± 0.2	0.8 ± 0.1	0.6 ± 0.1	0.5 ± 0.1	1.8 ± 0.2	1.3 ± 0.1	3.1 ± 0.2
Pr	1.0 ± 0.2	1.0 ± 0.2	1.2 ± 0.2	1.2 ± 0.2	–	0.6 ± 0.1	1.6 ± 0.1	0.9 ± 0.1	–
Nd	1.0 ± 0.2	0.7 ± 0.1	1.1 ± 0.1	1.2 ± 0.1	1.6 ± 0.1	0.9 ± 0.1	1.6 ± 0.2	1.0 ± 0.1	3.1 ± 0.2
Sm	1.1 ± 0.1	0.6 ± 0.1	1.1 ± 0.1	0.5 ± 0.1	–	0.5 ± 0.1	1.8 ± 0.2	1.0 ± 0.2	–
Eu	1.3 ± 0.2	0.5 ± 0.2	1.1 ± 0.2	2.3 ± 0.1	1.3 ± 0.1	–	1.4 ± 0.2	1.1 ± 0.2	–
Gd	1.1 ± 0.2	1.3 ± 0.4	1.0 ± 0.1	1.3 ± 0.1	1.4 ± 0.1	1.5 ± 0.1	1.7 ± 0.1	1.2 ± 0.1	–
Dy	–	0.6 ± 0.1	0.6 ± 0.1	0.3 ± 0.4	–	–	–	0.6 ± 0.1	4.9 ± 0.1

Table A1 – continued

	HD 210433	HD 211643	HD 211906	HD 215327	HD 220668	HD 223531	HD 224002	HD 224657
C	$-0.2 \pm 0.2$	–	$-0.3 \pm 0.1$	$-0.2 \pm 0.1$	–	$0.4 \pm 0.1$	$-0.3 \pm 0.1$	$0.5 \pm 0.1$
O	–	–	$-0.6 \pm 0.1$	$-0.4 \pm 0.1$	–	$0.2 \pm 0.1$	–	$0.7 \pm 0.1$
Na	–	$-0.7 \pm 0.1$	$-0.6 \pm 0.1$	$0.1 \pm 0.1$	–	$-0.1 \pm 0.4$	$-0.2 \pm 0.1$	$0.1 \pm 0.1$
Mg	$-0.4 \pm 0.1$	$0.3 \pm 0.1$	$0.3 \pm 0.1$	$1.0 \pm 0.1$	$-1.5 \pm 0.1$	$0.7 \pm 0.2$	$0.1 \pm 0.2$	$0.4 \pm 0.1$
Si	–	–	$0.3 \pm 0.2$	$0.7 \pm 0.1$	$0.5 \pm 0.1$	$0.9 \pm 0.1$	$0.2 \pm 0.3$	$0.3 \pm 0.1$
S	$1.1 \pm 0.1$	$0.0 \pm 0.3$	–	$0.8 \pm 0.1$	$0.3 \pm 0.1$	$-0.5 \pm 0.1$	–	$0.0 \pm 0.1$
Ca	$-0.1 \pm 0.1$	$-0.5 \pm 0.2$	$-0.3 \pm 0.1$	$0.4 \pm 0.2$	–	$0.1 \pm 0.1$	$-0.9 \pm 0.1$	$-0.7 \pm 0.2$
Sc	$-0.5 \pm 0.2$	$-1.2 \pm 0.2$	$0.4 \pm 0.2$	$-0.9 \pm 0.2$	–	$-1.4 \pm 0.2$	$-1.8 \pm 0.2$	$0.1 \pm 0.2$
Ti	$0.6 \pm 0.2$	$-0.1 \pm 0.1$	$0.3 \pm 0.1$	$0.7 \pm 0.2$	$-0.6 \pm 0.4$	$0.4 \pm 0.2$	$0.2 \pm 0.1$	$0.1 \pm 0.1$
V	$1.6 \pm 0.1$	$1.1 \pm 0.1$	$1.0 \pm 0.1$	$0.0 \pm 0.2$	$0.4 \pm 0.3$	$-0.7 \pm 0.2$	$0.7 \pm 0.2$	$-0.9 \pm 0.2$
Cr	$1.6 \pm 0.2$	$0.3 \pm 0.2$	$0.7 \pm 0.2$	$1.5 \pm 0.1$	$0.8 \pm 0.2$	$1.0 \pm 0.1$	$0.6 \pm 0.1$	$0.3 \pm 0.1$
Mn	$1.1 \pm 0.1$	$0.2 \pm 0.1$	$0.5 \pm 0.1$	$1.3 \pm 0.1$	$1.5 \pm 0.1$	$1.1 \pm 0.1$	$0.5 \pm 0.1$	$-0.4 \pm 0.2$
Fe	$1.0 \pm 0.1$	$0.3 \pm 0.1$	$0.8 \pm 0.2$	$1.4 \pm 0.1$	$0.3 \pm 0.2$	$1.0 \pm 0.1$	$0.6 \pm 0.1$	$0.4 \pm 0.1$
Co	–	–	$1.0 \pm 0.1$	–	–	–	$1.3 \pm 0.1$	$0.8 \pm 0.1$
Ni	$0.5 \pm 0.1$	$0.6 \pm 0.2$	$0.8 \pm 0.1$	$1.7 \pm 0.2$	$0.5 \pm 0.1$	$0.9 \pm 0.2$	$0.6 \pm 0.1$	$0.4 \pm 0.1$
Cu	–	–	$-0.1 \pm 0.2$	–	–	–	$-0.1 \pm 0.1$	$0.4 \pm 0.1$
Zn	$1.6 \pm 0.1$	–	$1.1 \pm 0.3$	$2.4 \pm 0.1$	–	$1.3 \pm 0.1$	$1.0 \pm 0.3$	$0.3 \pm 0.4$
Sr	$1.3 \pm 0.1$	$1.7 \pm 0.3$	$1.4 \pm 0.1$	$2.3 \pm 0.1$	$1.1 \pm 0.1$	$2.5 \pm 0.3$	$1.2 \pm 0.3$	$0.9 \pm 0.3$
Y	$1.9 \pm 0.1$	$-0.1 \pm 0.1$	$1.7 \pm 0.1$	$2.5 \pm 0.1$	–	$2.7 \pm 0.2$	$1.5 \pm 0.1$	$0.4 \pm 0.1$
Zr	$1.1 \pm 0.2$	$0.5 \pm 0.1$	$1.1 \pm 0.1$	$1.7 \pm 0.1$	$-0.1 \pm 0.4$	$1.8 \pm 0.1$	$1.1 \pm 0.2$	$0.4 \pm 0.1$
Ba	$-0.9 \pm 0.1$	$0.7 \pm 0.3$	$2.2 \pm 0.2$	$3.4 \pm 0.3$	–	$3.5 \pm 0.1$	$2.2 \pm 0.2$	$0.8 \pm 0.2$
La	–	–	$1.4 \pm 0.2$	–	–	–	$2.2 \pm 0.2$	$1.2 \pm 0.3$
Ce	$2.0 \pm 0.1$	$1.3 \pm 0.1$	$1.1 \pm 0.1$	$2.2 \pm 0.1$	–	$1.7 \pm 0.1$	$1.0 \pm 0.1$	$0.2 \pm 0.1$
Pr	–	–	–	$2.9 \pm 0.3$	–	–	$0.3 \pm 0.1$	$0.9 \pm 0.3$
Nd	$1.7 \pm 0.5$	–	$0.8 \pm 0.1$	$1.6 \pm 0.1$	$2.0 \pm 0.1$	$1.5 \pm 0.2$	$1.0 \pm 0.1$	$1.0 \pm 0.1$
Sm	$1.6 \pm 0.1$	–	$0.5 \pm 0.1$	$1.6 \pm 0.1$	–	$1.6 \pm 0.1$	$0.6 \pm 0.1$	$1.0 \pm 0.1$
Eu	–	–	$1.0 \pm 0.3$	$3.0 \pm 0.1$	–	–	$1.1 \pm 0.2$	$0.4 \pm 0.4$
Gd	$3.3 \pm 0.4$	$1.4 \pm 0.1$	$0.9 \pm 0.1$	$3.1 \pm 0.1$	–	$0.9 \pm 0.1$	$1.5 \pm 0.1$	$1.5 \pm 0.1$
Dy	$3.9 \pm 0.1$	$0.5 \pm 0.1$	–	$3.2 \pm 0.1$	–	$2.3 \pm 0.1$	–	–

This paper has been typeset from a  $\text{\TeX}/\text{\LaTeX}$  file prepared by the author.